Glycolysis-dependent Sulfur Metabolism Orchestrates Morphological Plasticity and Virulence in Fungi

Authors:
Dhrumi Shah[1,2], Nikita Rewatkar[1], Adishree M[1], Siddhi Gupta[1,2], Sudharsan Mathivathanan[1], Sayantani Biswas[1] and Sriram Varahan[1#]

Affiliations:
[1]CSIR-Centre for Cellular and Molecular Biology, Uppal Road, Hyderabad 500007, India.

[2]Academy of Scientific and Innovative Research (AcSIR), Ghaziabad- 201002, India.

- Corresponding Author:
Dr. Sriram Varahan
Senior Scientist
CSIR-Centre for Cellular and Molecular Biology (CCMB)
Email: sriram.ccmb@csir.res.in

Abstract

Fungi exhibit remarkable morphological plasticity, which allows them to undergo reversible transitions between distinct cellular states in response to changes in their environment. This phenomenon, termed fungal morphogenesis, is critical for fungi to survive and colonize diverse ecological niches and establish infections in a variety of hosts. Despite significant advancements in the field with respect to understanding the gene regulatory networks that control these transitions, the metabolic determinants of fungal morphogenesis remain poorly characterized. In this study, we uncover a previously uncharacterized, conserved dependency between central carbon metabolism and *de novo* biosynthesis of sulfur-containing amino acids that is critical for fungal morphogenesis, in two key fungal species. Using a multidisciplinary approach, we demonstrate that glycolytic flux is crucial to drive fungal morphogenesis in a cAMP-independent manner and perturbation of this pathway leads to a significant downregulation in the expression of genes involved in *de novo* biosynthesis of sulfur-containing amino acids. Remarkably, exogenous supplementation of sulfur-containing amino acids robustly rescues the morphogenesis defect induced by the perturbation of glycolysis in both *Saccharomyces cerevisiae* and *Candida albicans*, underscoring the pivotal role of *de novo* biosynthesis of sulfur-containing amino acid as a downstream effector of morphogenesis. Furthermore, a *C. albicans* mutant lacking the glycolytic enzyme, phosphofructokinase-1 (Pfk1) exhibited significantly reduced survival within *murine* macrophages and attenuated virulence in a *murine* model of systemic candidiasis. Overall, our work elucidates a previously uncharacterized coupling between glycolysis and sulfur metabolism that is critical for driving fungal morphogenesis, contributing to our understanding of this conserved phenomenon.

Key words: Fungal Morphogenesis, Glycolysis, *Saccharomyces cerevisiae, Candida albicans,* Virulence

Introduction

In response to changes in their environment, fungi exhibit remarkable morphological plasticity, allowing them to reversibly transition between specialized cell states. This inherent ability to rapidly adapt to the changes in their environment is essential for their survival and allows them to colonize diverse ecological niches including various host organisms (Gow et al., 2002; Lin et al., 2015; Naranjo-Ortiz and Gabaldón, 2019). This conserved phenomenon, of fungal morphogenesis, encompasses a plethora of morphological forms including pseudohyphae, hyphae, appressoria and fruiting bodies to name a few (Lin et al., 2015; Riquelme et al., 2018). Importantly, these morphological transitions in various pathogenic fungal species significantly influence their interaction with the respective host, impacting their overall ability to cause persistent infections (Min et al., 2020; Wang and Lin, 2012). Fungal morphogenesis is conserved across a plethora of fungal species and has profound implications with respect to fungal ecology, anti-fungal drug resistance and pathogenicity across a spectrum of hosts (Christensen, 1989; Puumala et al., 2024; Sexton and Howlett, 2006). Consequently, it has been a central focus of intense scientific investigation over the last several years (Lin et al., 2015; Riquelme et al., 2018). During dimorphic transitions in fungi, changes in cell shape is accompanied with changes in cell polarity, cell size and cell-cell adhesion and these changes are regulated by two major signalling pathways: the cAMP-PKA pathway and MAP kinase (MAPK) pathways. Both pathways are crucial for morphogenesis in fungal model systems including *Saccharomyces cerevisiae* and *Candida albicans*. In *S. cerevisiae*, the cAMP-PKA pathway is a critical regulatory cascade that controls cellular differentiation, such as pseudohyphal growth, in response to glucose availability. The glucose signal is transduced through two parallel mechanisms: The G-protein coupled receptor (GPCR) Gpr1-Gpa2 system and the intracellular Ras system. The activation of Ras is triggered by high glycolytic flux, which is directly controlled by the Hxt (Hexose Transporter) family dictating the precise rate of glucose import into the cell. Both the Gpr1-Gpa2 and Ras pathways activate the adenylate cyclase (Cyr1), leading to elevated intracellular cAMP levels. This cAMP binds to the regulatory subunit Bcy1, releasing and activating the catalytic Tpk subunits of Protein Kinase A (PKA). This PKA activation, driven primarily by Tpk2, promotes the shift to a filamentous morphology by inducing the expression of necessary genes required for pseudohyphal differentiation (Colombo et al., 1998; Lorenz et al., 2000; Xue et al., 1998). Similarly, this pathway drives the essential yeast to hyphal transition in *C. albicans*, often *via* the regulator Efg1 (Maidan et al., 2005). Concurrently, the MAPK (Mitogen-Activated Protein Kinase) pathway operates in parallel to the cAMP-PKA cascade and coordinates fungal morphogenesis in response to extracellular stress and nutrient signals. In *S. cerevisiae*, the Kss1 cascade is the key effector that drives pseudohyphal growth, predominantly activating under nitrogen-limiting conditions (Lorenz and Heitman, 1998). In the opportunistic fungal pathogen *C. albicans*, the homologous Cek1 pathway is indispensable for coordinating the complex hyphal development. Cek1 acts as a multifaceted sensor, by processing external morphogenetic cues and often engaging directly with the cell wall integrity system to ensure structural stability during the rapid yeast to hyphal transition. This pathway is a critical determinant of virulence, as its activation promotes the expression of adherence factors and ensures the formation of biofilms, enabling the fungus to colonize host tissues and resist immune response (Csank et al., 1998). The cAMP-PKA and MAPK pathways function in a parallel manner, engaging in significant crosstalk to integrate diverse environmental signals and coordinate a precise morphological response (Biswas et al., 2007; Kumar, 2021). While significant progress has been made in elucidating the intricate gene regulatory networks that govern these

morphological transitions (e.g., Genetic networks that orchestrate yeast to pseudohyphal differentiation in *S. cerevisiae* and yeast to hyphal differentiation in *C. albicans* have been well characterized (Nantel et al., 2002; Ryan et al., 2012)), a critical knowledge gap persists regarding the underlying metabolic determinants of fungal morphogenesis. Despite the recognized influence of nutrient availability on fungal morphogenesis (Broach, 2012; Fleck et al., 2011; Kumar, 2021), our understanding of the specific metabolic networks and their regulatory influence on morphogenetic switching in fungi remain incompletely characterized.

In this study, we employed *S. cerevisiae* and the human fungal pathogen, *C. albicans* to dissect the metabolic underpinnings of fungal morphogenesis, under nitrogen-limiting conditions, a known trigger for morphogenetic switching in these fungi (Csank et al., 1998; Gimeno et al., 1992). Our findings reveal a critical role for central carbon metabolism, particularly glycolysis, in facilitating the yeast to pseudohyphal transition in *S. cerevisiae* in a cAMP-PKA independent manner and the yeast to hyphal transition in *C. albicans*, both of which have been shown to be crucial for their nutrient foraging ability in diverse niches and the ability of *C. albicans* to successfully infect a host (Palková and Váchová, 2006; Thompson et al., 2011). Comparative transcriptomic analysis identified a conserved metabolic network crucial for these morphogenetic switching events under nitrogen-limiting conditions. Importantly, we observed that perturbations in glycolytic flux using pharmacological and genetic means, negatively impact the expression of genes involved in sulfur metabolism. Furthermore, our functional studies demonstrated that supplementation with sulfur-containing amino acids (cysteine or methionine), effectively rescued the morphogenetic defects resulting from glycolytic impairment, establishing a novel metabolic axis linking glycolysis and sulfur metabolism in the regulation of fungal morphogenesis. Finally, we investigated the implications of this glycolysis-dependent sulfur metabolism on the virulence of *C. albicans*. Our data demonstrates that a *C. albicans* mutant lacking genes that encode for a crucial glycolytic enzyme, phosphofructokinase-1 (Pfk1), exhibits reduced survival within macrophages and severely attenuated virulence in an *in vivo murine* model of systemic candidiasis which is rescued in response to sulfur supplementation to the host.

Collectively, our research, for the first time, identifies a previously uncharacterized metabolic axis linking glycolysis and sulfur metabolism under conditions that induce fungal morphogenesis and underscores the importance of this metabolic network in regulating fungal morphogenesis across two key fungal species and the ability of the human fungal pathogen, *C. albicans* to establish infection in a host. These findings address a fundamental knowledge gap in the field and contributes significantly to our understanding of a broadly conserved phenomenon that exists across a plethora of fungal species.

Results

Glycolysis is Critical for Pseudohyphal Differentiation in a cAMP-PKA Independent Manner in *S. cerevisiae*:

Nitrogen limitation is essential for yeast to pseudohyphal transition in *S. cerevisiae* (Gimeno et al., 1992; Pan et al., 2000). However, the influence of carbon sources on this phenomenon is not completely understood. It has been observed that fermetable carbon sources (sucrose, maltose, glucose, etc.) are important for inducing pseudohyphal differentiation under nitrogen-limiting conditions (Van De Velde and Thevelein, 2008).

199 Conversely, when these were replaced with non-fermentable carbon sources, there was a
200 significant reduction in pseudohyphal differentiation (Strudwick et al., 2010). This
201 indicates that the presence of fermentable carbon sources is critical for pseudohyphal
202 differentiation in *S. cerevisiae*. Crabtree positive organisms like *S. cerevisiae* metabolize
203 glucose primarily *via* glycolysis to meet their growth and energy demands (Barford and
204 Hall, 1979; De Deken, 1966). In order to determine whether the ability of
205 *S. cerevisiae* to metabolize glucose *via* glycolysis is critical for pseudohyphal differentiation
206 under nitrogen-limiting conditions, we spotted *S. cerevisiae* wild-type ∑1278b on nitrogen-
207 limiting media containing 2% glucose (SLAD) with and without sub-inhibitory
208 concentrations of 2-Deoxy-D-Glucose (2DG) and sodium citrate (NaCi), which are well
209 characterized glycolysis inhibitors (Cramer and Woodward, 1952; Evans and Ratledge,
210 1985; Yoshino and Murakami, 1982) and monitored pseudohyphal differentiation (Fig. 1A).
211 Our data demonstrates that sub-inhibitory concentrations of 2DG and NaCi significantly
212 attenuated the ability of *S. cerevisiae* to undergo pseudohyphal differentiation (Fig. 1B).
213 We then isolated cells from these colonies and quantified the percentage of pseudohyphal
214 cells (cells with a length/width ratio of 2 or more (Schröder et al., 2000)) in these colonies.
215 Addition of 2DG or NaCi resulted in a significant reduction in pseudohyphal cells (Fig. 1C)
216 without compromising the overall growth of *S. cerevisiae* wild-type ∑1278b (Fig. 1G).
217 Another diploid *S. cerevisiae* strain that is known to undergo pseudohyphal differentiation
218 under nitrogen-limiting conditions is the prototrophic CEN.PK strain (Laxman and Tu,
219 2011). In order to determine if our observations in ∑1278b can be recapitulated in CEN.PK,
220 *S. cerevisiae* wild-type CEN.PK was spotted on SLAD with and without sub-inhibitory
221 concentrations of 2DG or NaCi. Our data clearly demonstrates that 2DG and NaCi strongly
222 inhibit pseudohyphal differentiation (Fig. 1B and C) without compromising the overall
223 growth of *S. cerevisiae* wild-type CEN.PK as well (Fig. 1G).
224
225 Given that, 2DG and NaCi exhibited a strong inhibitory effect on pseudohyphal
226 differentiation under nitrogen-limiting conditions in a strain-independent manner, we
227 wanted to corroborate these observations by using pertinent genetic knockout strains that
228 are compromised in performing glycolysis, in the presence of glucose (Heinisch, 1986;
229 Smith et al., 2004). In order to do this, we generated knockout strains which lack the
230 genes that encode for enzymes that are involved in the glycolysis pathway including *pfk1*
231 (phosphofructokinase-1) and *adh1* (alcohol dehydrogenase-1) (Bennetzen and Hall, 1982;
232 Foy and Bhattacharjee, 1978) (Fig. 1D). Heinisch observed that a null mutant of *pfk1*, a
233 key glycolytic enzyme, is viable and can grow on glucose as a sole carbon source under
234 conditions where cell performs aerobic glycolysis. However, this same mutant exhibits a
235 significant growth defect when cultured anaerobically (Heinisch, 1986; Lobo and Maitra,
236 1983). Similarly, Dickinson et al., showed that a null mutant of *adh1* is viable. This is
237 likely due to the presence of multiple alcohol dehydrogenase isozymes present in
238 *S. cerevisiae* that likely compensate for the absence of *adh1* (Dickinson et al., 2003). The
239 deletions of *pfk1* and *adh1* genes were confirmed through whole genome sequencing
240 (Suppl.Fig. 1A and B). Our result demonstrates that the deletion of *pfk1* and *adh1* in the
241 ∑1278b background (*ΔΔpfk1* refers to the *pfk1* knockout strain and *ΔΔadh1* refers to the
242 *adh1* knockout strain) resulted in a significant reduction in pseudohyphal differentiation,
243 compared to the corresponding wild-type strain, under nitrogen-limiting conditions (Fig.
244 1E). We then isolated cells from these colonies and quantified the percentage of
245 pseudohyphal cells in these colonies. Deletion of *pfk1* and *adh1* resulted in a significant
246 reduction in pseudohyphal cells (Fig. 1F) corroborating our data obtained using the
247 glycolytic inhibitors, 2DG and NaCi. Similarly, deletion of *pfk1* and *adh1* in the CEN.PK
248 background resulted in a significant reduction in pseudohyphal differentiation (Fig. 1E and

F). In order to rule out whether the reduction in pseudohyphal differentiation in these mutants, is due to a general growth defect, we performed growth curve analysis wherein overnight grown cultures of the deletion strains (*ΔΔpfk1* and *ΔΔadh1)* along with wild-type strains (∑1278b or CEN.PK) were diluted to OD_{600}=0.01 in fresh SLAD and allowed to grow at 30 °C for 24 hours. OD_{600} was recorded at 3-h intervals (Fig. 1H). Our data suggests that the reduction in pseudohyphal differentiation is not due to general growth defect as the mutants were able to grow similar to the wild-type strains in SLAD (Fig. 1H). Taken together, our results clearly demonstrate that the ability of *S. cerevisiae* to efficiently metabolize glucose *via* glycolysis is critical for pseudohyphal differentiation under nitrogen-limiting conditions.

It is well-established that in *S. cerevisiae*, glucose acts as a key signalling molecule and is sensed by the G-protein coupled receptor, Gpr1 that activates the cAMP-PKA pathway, which in turn is crucial for pseudohyphal differentiation under nitrogen-limiting conditions (Lorenz, 1997; Lorenz et al., 2000). Additionally, a key glycolytic intermediate, fructose-1,6-bisphosphate (FBP), is also known to activate the cAMP-PKA pathway *via* activation of Ras proteins, further linking glucose metabolism to this crucial signalling cascade (Peeters et al., 2017) (Fig. 1I). To investigate whether the pseudohyphal differentiation defects that we observed due to glycolysis perturbation were solely due to the inability of glucose to activate the cAMP-PKA pathway, we performed cAMP add-back assays wherein *S. cerevisiae* wild-type ∑1278b was spotted on SLAD containing sub-inhibitory concentrations of 2DG or NaCi in the presence and absence of 1mM cAMP (Lorenz, 1997). Interestingly, the exogenous addition of cAMP failed to rescue pseudohyphal differentiation defect caused by the perturbation of glycolysis through 2DG or NaCi under nitrogen-limiting condition (Fig. 1J and L). We next asked if the exogenous addition of cAMP rescues the pseudohyphal differentiation defect exhibited by glycolysis defective strains, *ΔΔpfk1* and *ΔΔadh1*. In order to do this, we performed similar cAMP add-back assays wherein *S. cerevisiae* wild-type ∑1278b along with *ΔΔpfk1* and *ΔΔadh1* strains were spotted on SLAD in the presence and absence of 1mM cAMP. The *ΔΔgpa2* strain was used as a control because it is well-established that the deletion of *gpa2* (G protein that activates cAMP production in response to glucose (Rolland et al., 2000)) impairs pseudohyphal differentiation and this defect can be fully rescued by the exogenous addition of cAMP under nitrogen-limiting conditions (Harashima and Heitman, 2002; Lorenz, 1997). Corroborating our previous data, the exogenous addition of cAMP failed to rescue pseudohyphal differentiation defect caused by the perturbation of glycolysis *via* the deletion of *pfk1* and *adh1* but fully rescued the pseudohyphal differentiation defect exhibited by the *ΔΔgpa2* strain (Fig. 1K and L). Taken together, our results clearly demonstrate that the ability of *S. cerevisiae* to efficiently metabolize glucose *via* glycolysis is critical for pseudohyphal differentiation in a cAMP-PKA pathway independent manner under nitrogen-limiting conditions. This implies that glycolysis may be parallelly regulating other cellular processes essential for this morphological transition under nitrogen-limiting conditions.

Comparative Transcriptomics Identifies Glycolysis-dependent Regulation of Sulfur Metabolism During Pseudohyphal Differentiation in *S. cerevisiae*:

Our previous data showed that the perturbation of glycolysis using specific inhibitors including 2DG/NaCi or deletion of genes that encode for glycolytic enzymes including *pfk1/ adh1* resulted in a significant reduction in pseudohyphal differentiation in a cAMP-PKA independent manner, under nitrogen-limiting conditions (Fig. 1). Given that, glycolysis

strongly influences the global transcriptional landscape of *S. cerevisiae* (Newcomb et al., 2003; Wu et al., 2019), we undertook a comprehensive transcriptomic approach to identify the changes in the transcriptional landscape of *S. cerevisiae* colonies, in conditions that perturb glycolysis, resulting in the inhibition of pseudohyphal differentiation. We performed comparative RNA-Seq analysis using RNA isolated from wild-type cells spotted on SLAD in the presence and absence of the glycolysis inhibitor, 2DG (2DG addition was used to perturb glycolysis in our transcriptomics experiments, as it exerted the strongest inhibitory effect on pseudohyphal differentiation as shown in Fig. 1B and C). The experimental schematic is depicted in Fig. 2A. Briefly, comparative RNA-Seq analysis was done using wild-type colonies grown on SLAD in the presence and absence of 2DG isolated on day 5 (D-5) and day 10 (D-10), respectively (Fig. 2A). We have used D-5 as an early time point for our experiments, as we have consistently observed the emergence of pseudohyphae in colonies spotted on SLAD at this time-point and D-10 as a late time point wherein colonies exhibit robust pseudohyphal differentiation (Suppl.Fig. 2A). A volcano plot of differential gene expression in 2DG treated cells compared to untreated cells in both D-5 and D-10 is shown in Fig. 2B wherein some of the significantly upregulated and downregulated genes are highlighted with green colour. Previous studies in the field have shown that, under nitrogen-limiting/glucose-replete conditions, glycolytic intermediates provide various precursors needed for the biosynthesis of several amino acids in order to maintain amino acid homeostasis (Dikicioglu et al., 2011; Martíez-force and Benítez, 1992) and perturbation of glycolysis under these conditions results in the increased transcription of various genes involved in amino acid biosynthesis, as a feedback response. As expected, the expression of several genes involved in amino acid biosynthesis and transport were significantly upregulated in 2DG treated cells compared to untreated cells, in both D-5 and D-10 respectively (Suppl.Fig. 2B) corroborating the observations from the previously mentioned studies (Dikicioglu et al., 2011; Martíez-force and Benítez, 1992; Wu et al., 2004). Interestingly and rather unexpectedly, the expression of multiple genes specifically involved in the biosynthesis and transport of sulfur-containing amino acids, cysteine and methionine were significantly downregulated in 2DG treated cells compared to untreated cells in both D-5 and D-10 respectively (Fig. 2C). Our RNA-Seq analysis clearly demonstrates that multiple genes involved in the de novo biosynthesis of sulfur-containing amino acids, are significantly downregulated in the presence of 2DG, under nitrogen-limiting conditions.

Given that, perturbation of glycolysis *via* 2DG addition resulted in a clear downregulation of multiple genes involved in the *de novo* biosynthesis of sulfur-containing amino acids under nitrogen-limiting conditions, we wanted to corroborate these observations by using pertinent genetic knockout strains, *ΔΔpfk1* and *ΔΔadh1*. In order to determine this, we spotted *S. cerevisiae* wild-type ∑1278b along with *ΔΔpfk1* and *ΔΔadh1* on SLAD and cells from colonies were isolated after ~4 days for RNA isolation. We then performed comparative RT-qPCR to check for the relative expression of genes involved in *de novo* biosynthesis of sulfur-containing amino acids including *met32* (Zinc-finger DNA-binding transcription factor), *met3* (ATP sulfurylase), *met5* (Sulfite reductase beta subunit), and *met17* (O-acetyl homoserine-O-acetyl serine sulfhydrylase) (Blaiseau et al., 1997; Masselot and de Robichon-Szulmajster, 1975). Our data clearly shows that all the aforesaid genes were significantly downregulated in the *ΔΔpfk1* and *ΔΔadh1* strains compared to wild-type (Suppl.Fig. 2C) suggesting that genetic perturbation of glycolysis negatively impacts sulfur metabolism under nitrogen-limiting conditions.

348 In order to determine whether these observed trends are reflected at the protein level, we
349 generated strains wherein various proteins involved in the de novo biosynthesis of sulfur-
350 containing amino acids including Met4 (Leucine-zipper transcriptional activator), Met32
351 (Zinc-finger DNA-binding transcription factor), Met16 (3'-phosphoadenylsulfate
352 reductase), Met10 (Subunit alpha of assimilatory sulfite reductase), Cys4 (Cystathionine
353 beta-synthase) and Cys3 (Cystathionine gamma-lyase) were epitope-tagged (Fig. 2D).
354 These strains were spotted on SLAD in the presence and absence of 2DG following which,
355 cells from colonies were isolated on D-5 and levels of these proteins were assessed by
356 using Western blotting (Fig. 2E). Our results indicate that the levels of Met4, Met32, Met16,
357 Met10, Cys4 and Cys3 were significantly reduced in the 2DG treated cells compared to
358 untreated cells, corroborating our transcriptome data (Fig. 2E and Suppl.Fig. 3A). This
359 clearly demonstrates that perturbation of glycolysis negatively influences the expression
360 of sulfur metabolism proteins, under nitrogen-limiting conditions. We next asked, if the
361 glycolysis-dependent regulation of sulfur metabolism under nitrogen-limiting conditions
362 (SLAD) is restricted to conditions wherein cells physically attach to solid surfaces (colony
363 growth) or whether it is conserved even in conditions where cells are free-floating (liquid-
364 culture growth). In order to do this, pertinent epitope-tagged strains (wherein Met32,
365 Met16, Met10 and Cys3 were HA-tagged) were grown in liquid SLAD in the presence and
366 absence of 2DG for 24 hours after which the expression of the aforesaid proteins were
367 assessed using Western blotting (Suppl.Fig. 3B and C). Importantly, our results indicate
368 that the levels of Met32, Met16, Met10 and Cys3 were significantly reduced in the 2DG
369 treated cells compared to untreated cells (Suppl.Fig. 3B and C). Taken together, our data
370 clearly demonstrates that the perturbation of glycolysis under nitrogen-limiting conditions
371 negatively influences sulfur metabolism.
372
373 **Exogenous Supplementation of Sulfur Sources Rescues Pseudohyphal**
374 **Differentiation Defects Caused by the Perturbation of Glycolysis in *S. cerevisiae*:**
375
376 Our comparative transcriptomics data clearly demonstrates that, under nitrogen-limiting
377 conditions, glycolysis plays a critical role in regulating the expression of genes involved in
378 the *de novo* biosynthesis of sulfur-containing amino acids (Fig. 2). Based on our previous
379 data, we hypothesized that under nitrogen-limiting conditions, active glycolysis enables
380 *de novo* biosynthesis of sulfur-containing amino acids which in turn, is critical for
381 pseudohyphal differentiation and perturbation of active glycolysis using inhibitors like 2DG
382 or disruption of genes involved in glycolysis including *pfk1* or *adh1* negatively affects
383 glycolysis-mediated regulation of sulfur metabolism leading to attenuation of
384 pseudohyphal differentiation. If the proposed hypothesis holds true, the exogenous
385 supplementation of sulfur-containing compounds should mitigate the fungal
386 morphogenetic defects resulting from the perturbation of glycolysis. In order to test this,
387 we performed sulfur add-back assays wherein *S. cerevisiae* wild-type ∑1278b was spotted
388 on SLAD containing sub-inhibitory concentration of 2DG in the presence and absence of
389 sulfur-containing amino acids (cysteine or methionine). Remarkably, the exogenous
390 addition of cysteine resulted in a significant rescue of the pseudohyphal differentiation
391 defect observed in nitrogen-limiting medium containing 2DG (Fig. 3A). Corroborating this
392 observation, the percentage of pseudohyphal cells in colonies isolated from SLAD
393 containing 2DG and cysteine were significantly higher than the percentage of
394 pseudohyphal cells in colonies isolated from SLAD containing 2DG alone (Fig. 3B).
395 Interestingly, the addition of methionine failed to rescue the pseudohyphal differentiation
396 defects caused by the perturbation of glycolysis (Fig. 3A and B).
397

398 We next asked if the exogenous addition of sulfur sources rescues the pseudohyphal
399 differentiation defect exhibited by glycolysis defective strains, *ΔΔpfk1* and *ΔΔadh1*. In
400 order to do this, we performed similar sulfur add-back assays wherein *S. cerevisiae* wild-
401 type ∑1278b along with *ΔΔpfk1* and *ΔΔadh1* strains were spotted on SLAD in the presence
402 and absence of sulfur-containing amino acids (cysteine or methionine). The exogenous
403 addition of cysteine and methionine were able to significantly rescue the pseudohyphal
404 differentiation defect exhibited by the *ΔΔpfk1* and *ΔΔadh1* strains albeit at different levels
405 (Fig. 3C). Corroborating this observation, the percentage of pseudohyphal cells in *ΔΔpfk1*
406 and *ΔΔadh1* colonies isolated from SLAD containing cysteine or methionine were
407 significantly higher than the percentage of pseudohyphal cells in *ΔΔpfk1* and *ΔΔadh1*
408 colonies isolated from SLAD alone (Fig. 3D). Taken together, our results clearly
409 demonstrate that the glycolysis-mediated regulation of sulfur metabolism is critical for
410 pseudohyphal differentiation under nitrogen-limiting conditions.
411
412 **Sulfur Metabolism is Critical for Pseudohyphal Differentiation Under Nitrogen-**
413 **limiting Conditions in *S. cerevisiae*:**
414
415 Our previous observations strongly suggest a direct role for sulfur metabolism in regulating
416 fungal morphogenesis, under nitrogen-limiting conditions. In order to determine whether
417 glycolysis-dependent sulfur metabolism is critical for pseudohyphal differentiation, under
418 nitrogen-limiting conditions, we generated a knockout strain that lacks *met32* (gene that
419 encodes for a zinc-finger DNA-binding transcription factor involved in the regulation of *de*
420 *novo* biosynthesis of sulfur-containing amino acids (Blaiseau et al., 1997)). Unlike
421 deletions of most other genes involved in the *de novo* biosynthesis of sulfur-containing
422 amino acids, *met32* deletion strain does not exhibit auxotrophy for methionine or cysteine
423 (Blaiseau et al., 1997). This is likely due to the functional redundancy provided by its
424 paralog, *met31* (Blaiseau et al., 1997). We then assessed the ability of the *met32* deletion
425 strain to undergo pseudohyphal differentiation under nitrogen-limiting conditions. Deletion
426 of *met32* resulted in a significant reduction in pseudohyphal differentiation. Corroborating
427 this observation, the percentage of pseudohyphal cells in *ΔΔmet32* colonies were
428 significantly lower in SLAD, compared to *S. cerevisiae* wild-type ∑1278b colonies (Fig. 3E).
429 This suggests that perturbations to sulfur metabolism negatively affects pseudohyphal
430 differentiation. In order to rule out whether the reduction in pseudohyphal differentiation
431 in this mutant, is due to a general growth defect, we performed growth curve analysis
432 wherein overnight grown cultures of deletion strain (*ΔΔmet32)* along with wild-type strain
433 (∑1278b) were diluted to OD_{600}=0.01 in fresh SLAD and allowed to grow at 30 °C for 24
434 hours. OD_{600} was recorded at 3-h intervals (Suppl.Fig. 4A). Our data suggests that the
435 reduction in pseudohyphal differentiation is not due to general growth defect as the mutant
436 was able to grow similar to the wild-type strain in SLAD. We next asked if the exogenous
437 addition of sulfur sources rescues the pseudohyphal differentiation defect exhibited by
438 *ΔΔmet32*. In order to do this, we performed a simple sulfur add-back assay, wherein
439 *ΔΔmet32* strain was spotted on SLAD containing either cysteine or methionine and allowed
440 to undergo pseudohyphal differentiation. Our results show that the addition of cysteine or
441 methionine completely rescued the pseudohyphal differentiation defect exhibited by
442 *ΔΔmet32* strain. The percentage of pseudohyphal cells were also significantly higher in
443 *ΔΔmet32* colonies growing on SLAD containing cysteine or methionine compared to just
444 SLAD (Fig. 3F). Taken together, our data clearly demonstrates that the efficient *de novo*
445 biosynthesis of sulfur-containing amino acids including cysteine and methionine is critical
446 for pseudohyphal differentiation, under nitrogen-limiting conditions.
447

448 **Met30 is Involved in the Glycolysis-dependent Regulation of Sulfur Metabolism**
449 **During Pseudohyphal Differentiation in *S. cerevisiae*:**
450
451 Our previous data clearly demonstrates that, under nitrogen-limiting conditions, the levels
452 of Met4, a key activator of genes involved in the *de novo* biosynthesis of sulfur-containing
453 amino acids, was significantly reduced in 2DG treated cells compared to untreated cells
454 (Fig. 2E). Met4 activity is known to be negatively regulated by SCF^{Met30} (Skp1/Cullin1/F-
455 box) ubiquitin ligase complex in *S. cerevisiae* (Rouillon et al., 2000). Under sulfur-replete
456 conditions, Met30 promotes Met4 ubiquitination and degradation, thereby repressing the
457 *MET* gene network. Conversely, sulfur limitation reduces Met30 activity, allowing Met4 to
458 become active and induce the expression of genes required for sulfur amino acid
459 biosynthesis (Smothers et al., 2000). It is important to note that deletion of *met30* is
460 lethal in haploid strains of *S. cerevisiae* (Kaiser et al., 1998). While point mutations or
461 temperature sensitive *met30* mutants are commonly used in haploid strains to circumvent
462 this lethality (Kaiser et al., 1998; Su et al., 2008), our study in diploid *S. cerevisiae*
463 involved generating a heterozygous viable *met30* (*Δmet30*) deletion strain. In order to
464 confirm that the deletion of a single copy of *met30* does not lead to any growth defects in
465 SLAD, we performed growth curve analysis wherein overnight grown cultures of deletion
466 strain (*Δmet30)* along with wild-type strain (∑1278b) were diluted to OD_{600}=0.01 in fresh
467 SLAD and allowed to grow at 30 °C for 24 hours. OD_{600} was recorded at 3-h intervals
468 (Suppl.Fig. 4A). Our data suggests that the deletion of *met30* does not affect overall
469 growth as the mutant was able to grow similar to the wild-type strain in SLAD (Suppl.Fig.
470 4A). Based on our previous data, we hypothesized that under nitrogen-limiting conditions,
471 active glycolysis enables *de novo* biosynthesis of sulfur-containing amino acids by reducing
472 the activity of Met30. Conversely, we hypothesized that perturbing active glycolysis with
473 glycolysis inhibitor, 2DG increases Met30 activity, which in turn inactivates Met4, thereby
474 negatively affecting *MET* gene transcription, ultimately resulting in attenuated
475 pseudohyphal differentiation (Fig. 3G). In order to investigate this hypothesis, we
476 generated strains wherein one copy of *met30* was deleted and various proteins involved
477 in the *de novo* biosynthesis of sulfur-containing amino acids including Met4 (Leucine-zipper
478 transcriptional activator), Met32 (Zinc-finger DNA-binding transcription factor), Met16 (3'-
479 phosphoadenylsulfate reductase) and Cys3 (Cystathionine gamma-lyase) were epitope-
480 tagged. These strains were spotted on SLAD in the presence and absence of 2DG following
481 which, cells from colonies were isolated on D-5 and levels of these proteins were assessed
482 by using Western blotting. Our results indicate that the levels of Met4, Met32, Met16 and
483 Cys3 were similar in both 2DG treated and untreated cells, in the *Δmet30* deletion strain
484 (Fig. 3H and I). This suggests that glycolysis influences Met30 activity which in turn
485 regulates Met4 activity thereby affecting the expression of genes involved in the *de novo*
486 biosynthesis of sulfur-containing amino acids, under nitrogen-limiting conditions.
487
488 Based on our previous observation that 2DG treatment significantly reduces Met4 levels
489 in nitrogen-limiting conditions, (an effect that was notably absent in *met30* deletion
490 strains), we hypothesized that the 2DG-induced downregulation of Met4 is mediated by
491 an increase in Met30 levels. In order to check Met30 levels in the presence of 2DG, we
492 generated a strain wherein Met30 was epitope-tagged and this strain was spotted on
493 SLAD, in the presence and absence of 2DG following which, cells from colonies were
494 isolated on D-5 and levels of Met30 were assessed by using Western blotting. Our results
495 indicate that the levels of Met30 were similar in both 2DG treated and untreated cells (Fig.
496 3J), suggesting that glycolysis influences Met30 activity post-translationally rather than

through changes in its protein abundance. Collectively, our findings indicate that the perturbation of glycolysis under nitrogen-limiting conditions negatively impacts sulfur metabolism through a mechanism dependent on Met30 activity.

Glycolysis-dependent Sulfur Metabolism is Critical for Hyphal Differentiation in *C. albicans*:

C. albicans is an opportunistic fungal pathogen that exhibits a remarkable degree of fungal morphogenesis in response to various environmental cues (Huang, 2012). Yeast to hyphal differentiation in *C. albicans* is well studied. However, we do not have a complete understanding of fundamental metabolic drivers that orchestrate this phenomenon. Given that central carbon metabolic pathways including glycolysis are well conserved across a plethora of fungal species including *C. albicans* (Askew et al., 2009) and nitrogen limitation is one of the key triggers for yeast to hyphal differentiation in *C. albicans* (Csank et al., 1998), we wanted to determine if glycolysis-mediated sulfur metabolism plays an important role in this morphogenetic switching in *C. albicans* as well. First, we wanted to understand whether the ability of C. *albicans* cells to metabolize glucose, under nitrogen-limiting conditions is critical for fungal morphogenesis (Fig. 4A). In order to do this, *C. albicans* wild-type SC5314 was spotted on SLAD, in the presence and absence of sub-inhibitory concentration of glycolysis inhibitor, 2DG, allowed to grow for 7 days, and cells were isolated and imaged using bright-field microscopy. Our data clearly demonstrates that sub-inhibitory concentration of 2DG significantly reduced filamentation in *C. albicans* (Fig. 4B) without compromising the overall growth of *C. albicans* wild-type SC5314 (Fig. 4H). We then isolated cells from these colonies and quantified the percentage of hyphal cells (cells with a length/width ratio of 4.5 or more (Su et al., 2018)) in these colonies. Corroborating our microscopy data, the percentage of hyphal cells in colonies spotted on SLAD containing 2DG was significantly lower compared to the percentage of hyphal cells in colonies spotted on SLAD without 2DG (Fig. 4B). To investigate whether the hyphal differentiation defects that we observed due to glycolysis perturbation were solely due to the inability of glucose to activate the cAMP-PKA pathway, we performed cAMP add-back assays wherein *C. albicans* wild-type SC5314 was spotted on SLAD containing sub-inhibitory concentrations of 2DG in the presence and absence of 5mM cAMP. Interestingly, corroborating our *S. cerevisiae* data, the exogenous addition of cAMP failed to rescue hyphal differentiation defect caused by the perturbation of glycolysis through 2DG under nitrogen-limiting condition in *C. albicans* (Suppl.Fig. 5B). Taken together, our results show that the ability of *C. albicans* to metabolize glucose is critical for fungal morphogenesis in a cAMP-PKA pathway independent manner under nitrogen-limiting conditions.

Given that the perturbation of glycolysis under nitrogen-limiting conditions, using 2DG exhibited a strong inhibitory effect on hyphal differentiation in *C. albicans* (Fig. 4B), similar to what we observed in *S. cerevisiae*, we wanted to determine if the expression of genes involved in the *de novo* biosynthesis of sulfur-containing amino acids are affected when glycolysis is perturbed in *C. albicans*, under nitrogen-limiting conditions (similar to what we observed in *S. cerevisiae*). In order to determine this, we spotted *C. albicans* wild-type SC5314 on SLAD, in the presence and absence of 2DG and cells from colonies were isolated after ~4 days for RNA isolation. We then performed comparative RT-qPCR to check for the relative expression of genes involved in *de novo* biosynthesis of sulfur-containing amino acids including *met32* (DNA-binding transcription factor), *met3* (ATP sulfurylase), *met5* (*ecm17*) (Sulfite reductase beta subunit), *met10* (Sulfite reductase), and *met17* (*met15*) (O-acetyl homoserine-O-acetyl serine sulfhydrylase) (Chebaro et al., 2017; Li et al., 2013;

547 Shrivastava et al., 2021), in cells isolated from colonies grown on SLAD containing 2DG
548 compared to cells isolated from colonies grown on SLAD without 2DG (Fig. 4C). Our data
549 clearly shows that all the aforesaid genes involved in *de novo* biosynthesis of sulfur-
550 containing amino acids pathway including *met32*, *met3*, *met5* (*ecm17*), *met10* and *met17*
551 (*met15*) were significantly downregulated in the presence of 2DG (Fig. 4D) suggesting
552 that perturbation of glycolysis negatively impacts sulfur metabolism in *C. albicans*, under
553 nitrogen-limiting conditions. To determine if the significant reduction in hyphal
554 differentiation that we observed in the presence of 2DG can be attributed to the reduced
555 expression of genes involved in the *de novo* biosynthesis of sulfur-containing amino acids,
556 we performed sulfur add-back assays similar to what was done in *S. cerevisiae* (Fig. 3A),
557 wherein *C. albicans* wild-type SC5314 was spotted on SLAD containing 2DG in the
558 presence and absence of cysteine or methionine, allowed to grow for 7 days, and cells
559 were isolated and imaged using bright-field microscopy. The addition of cysteine or
560 methionine significantly rescued hyphal differentiation defects in the presence of 2DG (Fig.
561 4E and F). We then isolated cells from these colonies and quantified the percentage of
562 hyphal cells. Corroborating our microscopy data, the percentage of hyphal cells in colonies
563 spotted on SLAD containing 2DG with cysteine or methionine were significantly higher
564 compared to the percentage of hyphal cells in colonies spotted on SLAD with 2DG alone
565 (Fig. 4E and F).
566
567 Our previous results clearly demonstrate that glycolysis and glycolysis-dependent sulfur
568 metabolism is critical for fungal morphogenesis of *C. albicans*, under nitrogen-limiting
569 conditions. In order to corroborate these observations by using pertinent genetic knockout
570 strains that are compromised in performing glycolysis, we generated a double knockout
571 strain lacking the gene that encodes for the glycolytic enzyme, phosphofructokinase-1
572 (Pfk1) using the SAT-Flipper method (Reuß et al., 2004). The deletion of *pfk1* was
573 confirmed through whole genome sequencing (Suppl.Fig. 5A). We then tested the ability
574 of this deletion strain to undergo hyphal differentiation under nitrogen-limiting conditions.
575 Briefly, *C. albicans* wild-type SC5314 and *ΔΔpfk1* were spotted on SLAD, allowed to grow
576 for 7 days, and cells were isolated and imaged using bright-field microscopy. Our result
577 shows that the *ΔΔpfk1* strain exhibits a significant reduction in hyphal differentiation
578 compared to *C. albicans* wild-type SC5314, under nitrogen-limiting conditions (Fig. 4G).
579 We then isolated cells from these colonies and quantified the percentage of hyphal cells in
580 these colonies. Corroborating our microscopy data, the percentage of hyphal cells in
581 *C. albicans* wild-type SC5314 colonies spotted on SLAD were significantly higher compared
582 to the percentage of hyphal cells in *ΔΔpfk1* colonies (Fig. 4G). In order to rule out whether
583 the reduction in hyphal differentiation in this mutant, is due to a general growth defect,
584 we performed growth curve analysis wherein overnight grown cultures of deletion strain
585 (*ΔΔpfk1)* along with wild-type strain (SC5314) were diluted to OD_{600}=0.01 in fresh SLAD
586 and allowed to grow at 30 °C for 24 hours. OD_{600} was recorded at 3-h intervals. Our data
587 suggests that the reduction in hyphal differentiation is not due to general growth defect
588 as the mutant was able to grow similar to the wild-type strain in SLAD (Fig. 4H). We next
589 asked if the exogenous addition of cAMP rescues the hyphal differentiation defect exhibited
590 by glycolysis defective strain, *ΔΔpfk1*. In order to do this, we performed similar cAMP add-
591 back assays wherein *C. albicans* wild-type SC5314 along with *ΔΔpfk1* strain were spotted
592 on SLAD in the presence and absence of 5mM cAMP. Corroborating our previous data, the
593 exogenous addition of cAMP failed to rescue hyphal differentiation defect caused by the
594 perturbation of glycolysis *via* the deletion of *pfk1* (Suppl.Fig. 5C).
595

596 In order to determine if the expression of genes involved in the *de novo* biosynthesis of
597 sulfur-containing amino acids are affected in *ΔΔpfk1*, under nitrogen-limiting conditions
598 (similar to what we observed in the presence of 2DG (Fig. 4D)), we spotted *C. albicans*
599 wild-type SC5314 and *ΔΔpfk1* on SLAD and cells from colonies were isolated after ~4
600 days, for RNA isolation. We then performed comparative RT-qPCR to check for the relative
601 expression of genes involved in *de novo* biosynthesis of sulfur-containing amino acids
602 including *met32* (DNA-binding transcription factor), *met3* (ATP sulfurylase), *met5* (*ecm17*)
603 (Sulfite reductase beta subunit), *met10* (Sulfite reductase) and *met17* (*met15*) (O-acetyl
604 homoserine-O-acetyl serine sulfhydrylase) (Chebaro et al., 2017; Li et al., 2013;
605 Shrivastava et al., 2021)(Fig. 4C). Our data clearly shows that all the aforesaid genes
606 involved in *de novo* biosynthesis of sulfur-containing amino acids pathway including
607 *met32*, *met3*, *met5* (*ecm17*), *met10* and *met17* (*met15*) were significantly downregulated
608 in *ΔΔpfk1* compared to the wild-type (Fig. 4I) suggesting that the genetic perturbation of
609 glycolysis negatively impacts sulfur metabolism in *C. albicans*, under nitrogen-limiting
610 conditions.
611
612 Our RT-qPCR results showed that the, deletion of *pfk1*, negatively influences sulfur
613 metabolism and this in turn might be causal for the reduced hyphal differentiation
614 observed in these conditions. Given this, we wanted to determine if the hyphal
615 differentiation defect exhibited by *ΔΔpfk1* can be rescued by the addition of sulfur-
616 containing amino acids. In order to do this, we performed sulfur add-back assays wherein
617 *ΔΔpfk1* strain was spotted on SLAD in the presence and absence of cysteine or methionine,
618 allowed to grow for 7 days and imaged using bright field microscopy. Interestingly, our
619 data shows that cysteine or methionine were able to rescue the hyphal differentiation
620 defect exhibited by the *ΔΔpfk1* strain (Fig. 4J and K). We then isolated cells from these
621 colonies and quantified the percentage of hyphal cells. Corroborating our microscopy data,
622 the percentage of hyphal cells in *ΔΔpfk1* colonies spotted on SLAD containing cysteine or
623 methionine were significantly higher compared to the percentage of hyphal cells in *ΔΔpfk1*
624 colonies spotted on SLAD alone (Fig. 4J and K). Overall, our data suggests that glycolysis-
625 mediated regulation of sulfur metabolism is critical for hyphal differentiation of *C. albicans*,
626 under nitrogen-limiting conditions highlighting the remarkable similarities with respect to
627 the regulation of fungal morphogenesis, between *S. cerevisiae* and *C. albicans*.
628
629 **Perturbation of Glycolysis Leads to Attenuated Fungal Virulence in *C. albicans***
630 **which is Rescued by Sulfur Supplementation:**
631
632 Several studies have established the importance of fungal morphogenesis as a key
633 virulence strategy used by *C. albicans* to establish successful infections in the host
634 (Gow et al., 2012; Moyes et al., 2016; Wilson et al., 2016). Based on our previous
635 observations that perturbation of glycolysis, either through 2DG treatment or deletion of
636 *pfk1* (*ΔΔpfk1*), significantly attenuates hyphal differentiation, we hypothesized that this
637 observed phenotype could be a consequence of transcriptional downregulation of genes
638 associated with hyphal differentiation and virulence. In order to test this hypothesis, we
639 spotted *C. albicans* wild-type SC5314 on SLAD, in the presence and absence of 2DG or
640 wild-type along with *ΔΔpfk1* on SLAD. Cells from colonies were isolated after ~4 days for
641 RNA isolation. We then performed comparative RT-qPCR to check for the relative
642 expression of genes involved in hyphal differentiation and virulence including *als3* (Cell
643 wall adhesin), *ece1* (Candidalysin), *hwp1* (Hyphal cell wall protein), *hyr1* (GPI-anchored
644 hyphal cell wall protein), *ihd1* (GPI-anchored protein), *rbt1* (Cell wall protein) and *sap6*
645 (Secreted aspartyl protease) (Bailey et al., 1996; Deorukhkar, 2017; Liu and Filler, 2011;

Martin et al., 2013; Monniot et al., 2013; Moyes et al., 2016; Richardson et al., 2018; Sharkey et al., 1999) (Fig. 5A). Our data clearly shows that all the aforesaid genes involved in hyphal differentiation and virulence including *als3, ece1, hwp1, hyr1, ihd1, rbt1* and *sap6* were significantly downregulated in both 2DG treated cells and in *ΔΔpfk1* suggesting that perturbation of glycolysis negatively affects the expression of genes involved in hyphal differentiation and virulence in *C. albicans*, under nitrogen-limiting conditions (Fig. 5B).

Given that *ΔΔpfk1*, displayed a significant attenuation in its ability to undergo hyphal differentiation and it had significantly reduced expression of genes associated with hyphal differentiation and virulence, we wanted to determine if this deletion strain was compromised in its ability to infect the host. In order to do this, we took a two-pronged approach wherein, we first tested the ability of the *ΔΔpfk1* strain to survive the harsh intracellular environment of the macrophages which *C. albicans* encounters during various stages of host infection (Jiménez-López and Lorenz, 2013; May and Casadevall, 2018; Uwamahoro et al., 2014). We performed an *in vitro* microbial survival assay wherein *RAW 264.7* macrophages were incubated either with *C. albicans* wild-type SC5314 or the *ΔΔpfk1* strain for one hour following which macrophages were lysed and fungi were serially diluted and plated to determine the viable population of the *C. albicans* wild-type SC5314 and the *ΔΔpfk1* strain (Fig. 5C). We also calculated the percentage of the wild-type or mutant strain that survived the incubation with the macrophages. Our results demonstrate that the viable population of *ΔΔpfk1* strain was significantly lower compared to the wild-type strain, after incubation with the macrophages (Fig. 5C). Similarly, the percentage survival of the *ΔΔpfk1* strain was significantly lower than the wild-type SC5314 (Fig. 5C). Overall, this data indicates that the *ΔΔpfk1* strain is compromised with respect to macrophage survival.

Given that the *ΔΔpfk1* strain was significantly attenuated in the macrophage survival assay, we next wanted to test the ability of this deletion strain to establish systemic infection in a host. In order to do this, we challenged healthy wild-type C57BL/6 mice intravenously with a dose of 1×10^7 CFU (lethal dose (Hirayama et al., 2020)) of *C. albicans* wild-type SC5314 or *ΔΔpfk1* strain *via* lateral tail vein injection. This is an established *murine* model of systemic candidiasis in the field and faithfully mimics the infection that occurs in humans (Segal and Frenkel, 2018). We then monitored survival of the infected animals for 21 days. Mice challenged with *ΔΔpfk1* strain had significantly increased survival compared to mice challenged with *C. albicans* wild-type SC5314 (Fig. 5D). *C. albicans* exhibits strong tropism towards kidneys during *murine* infections (Lionakis et al., 2011; Pappas et al., 2018) and in order to measure the fungal burden within the host, kidneys from C57BL/6 mice infected with both *C. albicans* wild-type SC5314 and *ΔΔpfk1* were harvested ~2 days post infection (when the mice injected with wild-type *C. albicans* SC5314 becomes moribund), homogenized and plated to measure the fungal burden by enumerating the colony forming units (CFU) (Fig. 5E). Our data indicates that kidneys isolated from mice challenged with the *ΔΔpfk1* strain had significantly lesser CFU compared to kidneys isolated from mice challenged with the *C. albicans* wild-type SC5314 (Fig. 5F). We also performed histological analysis on the infected kidneys using GMS staining (Grocott Methenamine Silver staining), to visualize the fungi (stained black) in the tissue. Kidneys isolated from mice challenged with the *C. albicans* wild-type SC5314 had higher amounts of fungi compared to kidneys isolated from mice challenged with the *ΔΔpfk1* strain (Fig. 5G). Overall, our data indicates that the perturbation of glycolysis significantly attenuates *C. albicans* virulence.

696 Our previous *in vitro* results clearly demonstrated that exogenous supplementation of
697 cysteine and methionine significantly rescued the hyphal differentiation defect exhibited
698 by *ΔΔpfk1* strain. Based on this, we wanted to check whether sulfur supplementation could
699 also rescue the virulence defects exhibited by *ΔΔpfk1*, in a *murine* model of systemic
700 candidiasis. Given that N-acetyl cysteine (NAC) is a commonly used exogenous sulfur
701 source for *in vivo* studies (Shee et al., 2022), we supplemented distilled water with NAC
702 (6mg/ml concentration) and this was administered to mice orally 72 hours prior to
703 infection. After 72 hours of pre-treatment with NAC, we challenged healthy wild-type
704 C57BL/6 mice intravenously with a dose of 1×10^7 CFU of wild-type SC5314 or *ΔΔpfk1*
705 strain *via* lateral tail vein injection (Fig. 5H). We then monitored survival of the infected
706 animals for 21 days. Remarkably, mice administered with NAC containing distilled water
707 had significantly reduced survival compared to mice administrated with normal distilled
708 water (Fig. 5I). We also performed histological analysis on the infected kidneys using GMS
709 staining, to visualize the fungi in the tissue. Kidneys isolated from mice administered with
710 NAC containing distilled water and infected with *ΔΔpfk1* had significantly higher amounts
711 of fungi compared to mice administrated with normal distilled water (Fig. 5J). This clearly
712 demonstrates that exogenous sulfur supplementation to the host *via* NAC administration,
713 reverses the attenuated virulence exhibited by the *ΔΔpfk1* strain.
714
715 **Discussion**
716
717 Our findings provide compelling evidence for a conserved metabolic network that
718 intricately links central carbon metabolism (particularly glycolysis), sulfur amino acid
719 biosynthesis, and fungal morphogenesis in both *Saccharomyces cerevisiae* and *Candida*
720 *albicans*. While nitrogen limitation is a well-established and essential trigger for the yeast
721 to pseudohyphae transition in *S. cerevisiae*, the specific influence of carbon sources on
722 this process has not been completely understood. Studies have shown that fermentable
723 carbon sources are critical for inducing pseudohyphal differentiation under nitrogen-
724 limiting conditions (Van De Velde and Thevelein, 2008). Conversely, when these
725 fermentable sugars are replaced with non-fermentable carbon sources, a significant
726 reduction in pseudohyphal differentiation is observed (Strudwick et al., 2010). These
727 findings collectively suggest that the presence of fermentable carbon sources, and by
728 extension their metabolism, is a critical requirement for inducing fungal morphogenesis in
729 *S. cerevisiae*. Glucose in the extracellular environment can be sensed by *S. cerevisiae*
730 using multiple proteins. One such protein is the well characterized G-protein coupled
731 receptor (GPCR), Gpr1. Binding of glucose to Gpr1 activates a downstream signalling
732 cascade, resulting in the production of cAMP which activates Protein Kinase A (PKA)
733 (Kraakman et al., 1999; Yun et al., 1997). This glucose-dependent cAMP-PKA pathway
734 has been shown to be essential for pseudohyphal differentiation under nitrogen-limiting
735 conditions (Lorenz et al., 2000). Additionally, a key glycolytic intermediate, fructose-1,6-
736 bisphosphate (FBP), is also known to activate the cAMP-PKA pathway *via* activation of Ras
737 proteins, further linking glucose metabolism to this crucial signalling cascade (Peeters et
738 al., 2017). However, the role of glucose as a metabolite in the context of pseudohyphal
739 differentiation is not known. Building upon previous data that fermentable carbon sources
740 that are metabolized *via* glycolysis are able to induce fungal morphogenesis, we asked
741 whether the ability of these cells to undergo active glycolysis is critical for fungal
742 morphogenesis. We took a two-pronged approach which involved pharmacological or
743 genetic perturbation of glycolysis, to address this question. Our findings clearly
744 demonstrated that active glycolysis is essential for fungal morphogenesis under nitrogen-
745 limiting conditions. To understand whether the pseudohyphal differentiation defects we

observed due to glycolysis perturbation were solely due to the inability of glucose to activate glucose-dependent cAMP-PKA pathway, we performed cAMP add-back assays and interestingly, exogenous supplementation of cAMP failed to rescue pseudohyphal differentiation defects caused by the perturbation of glycolysis (through inhibitors (2DG and NaCi) or through genetic knockout strains (*ΔΔpfk1* and *ΔΔadh1*)). Our results clearly demonstrate that the ability of *S. cerevisiae* to efficiently metabolize glucose *via* glycolysis is critical for pseudohyphal differentiation under nitrogen-limiting conditions, in a cAMP-PKA independent manner. This implies that glycolysis may be parallelly regulating other cellular mechanisms essential for this morphological transition. It is plausible that the glycolytic flux, or a yet to be identified downstream intermediate, acts as a distinct metabolic signal that is parallelly important for pseudohyphal differentiation along with the cAMP-PKA pathway. This uncovers a previously unrecognized layer of regulatory complexity in the interplay between central carbon metabolism and fungal morphogenesis.

To gain deeper insights underlying the glycolysis-mediated regulation of fungal morphogenesis in a cAMP-PKA independent manner, we performed comparative transcriptomics on *S. cerevisiae* wild-type cells grown under nitrogen-limiting conditions with and without the glycolysis inhibitor, 2DG (which had the strongest inhibitory effect on pseudohyphal differentiation). As anticipated, genes involved in amino acid biosynthesis and transport were upregulated in the 2DG treated cells, consistent with a feedback response that cells exhibits when glycolysis is perturbed under nitrogen-limiting conditions, as various intermediates of glycolysis are known to serve as precursors for the biosynthesis of several amino acids under these conditions (Dikicioglu et al., 2011; Martíez-force and Benítez, 1992). Remarkably, we observed a striking and unexpected downregulation of multiple genes specifically involved in the biosynthesis and transport of sulfur-containing amino acids, cysteine and methionine, in the 2DG treated cells at both early and late time points of pseudohyphal development. This transcriptional downregulation was further validated at the protein level for key proteins involved in the sulfur assimilation pathway (Met4, Met32, Met16, Met10, Cys4 and Cys3), clearly demonstrating the dependence of sulfur metabolism on active glycolysis during fungal morphogenesis. This unexpected link between central carbon metabolism and sulfur metabolism is not restricted to conditions that induce fungal morphogenesis *i.e.* in surface-attached colonies grown in nitrogen-limiting conditions since even in liquid cultures that have limiting levels of nitrogen, wherein *S. cerevisiae* cells do not undergo pseudohyphal differentiation (Gancedo, 2001; Gimeno et al., 1992), perturbation of glycolysis with 2DG results in significantly reduced expression of proteins involved in the sulfur assimilation pathway (Met32, Met16, Met10 and Cys3).

Given that multiple genes that encode for proteins involved in *de novo* biosynthesis of sulfur-containing amino acids were downregulated in the presence of 2DG, which strongly inhibits fungal morphogenesis, we wanted to explore the possibility that perturbation of sulfur metabolism is causal for the attenuation of fungal morphogenesis in the presence of 2DG. We tested the functional relevance of this glycolysis-dependent regulation of sulfur metabolism in fungal morphogenesis directly through exogenous supplementation of sulfur sources. Interestingly, cysteine specifically rescued the pseudohyphal differentiation defect exhibited by *S. cerevisiae* in the presence of 2DG. However, methionine was unable to rescue the pseudohyphal differentiation defect, in the presence of 2DG even at various different concentrations (50μM, 100 μM, 200μM and 500μM). The observed differential rescue effects of cysteine and methionine could be due to the distinct amino acid transport systems used by *S. cerevisiae* to transport these amino acids. *S. cerevisiae* primarily uses

796 multiple, low-affinity permeases (Gap1, Bap2, Bap3, Tat1, Tat2, Agp1, Gnp1, Yct1) for
797 cysteine transport, while relying on a limited set of high-affinity transporters (like Mup1)
798 for methionine transport, with the added complexity that its methionine transporters can
799 also transport cysteine (Düring-Olsen et al., 1999; Huang et al., 2017; Kosugi et al., 2001;
800 Menant et al., 2006). Hence, it is likely that cysteine uptake could be happening at a higher
801 efficiency in *S. cerevisiae* compared to methionine uptake. Therefore, to achieve a
802 comparable functional rescue by exogenous supplementation of methionine, it is necessary
803 to use a higher concentration of methionine. When we performed our rescue experiments
804 using higher concentrations of methionine, we did not see any rescue of pseudohyphal
805 differentiation in the presence of 2DG and in fact we noticed that, at higher concentrations
806 of methionine, the wild-type strain failed to undergo pseudohyphal differentiation even in
807 the absence of 2DG. This is likely due to the fact that increasing the methionine
808 concentration raises the overall nitrogen content of the medium, thereby making the
809 medium less nitrogen-starved. This presents a major experimental constraint, as
810 pseudohyphal differentiation is strictly dependent on nitrogen limitation, and the elevated
811 nitrogen resulting from the higher methionine concentration can inhibit pseudohyphal
812 differentiation. Similarly, gene expression analysis using RT-qPCR revealed a
813 significant downregulation of multiple genes involved in the biosynthesis of sulfur-
814 containing amino acids (*met32*, *met3, met5* and *met17)* in *ΔΔpfk1* and *ΔΔadh1* strains
815 and the pseudohyphal differentiation defects observed in these strains were completely
816 rescued by the addition of cysteine or methionine. These findings strongly implicate that
817 *de novo* biosynthesis of sulfur-containing amino acids is a critical downstream effector of
818 glycolytic activity in promoting pseudohyphal differentiation under nitrogen limitation. To
819 directly assess the role of sulfur metabolism in fungal morphogenesis, we generated and
820 characterized the *met32* deletion strain. This particular strain was critical for our
821 investigation because, unlike other *MET* gene deletions, *met32* deletion does not result in
822 auxotrophy for methionine or cysteine. This unique characteristic is attributed to the
823 functional redundancy provided by its paralog, *met31* (Blaiseau et al., 1997). The deletion
824 of *met32* resulted in substantial defects in pseudohyphal differentiation under nitrogen-
825 limiting conditions, directly implicating the role of sulfur metabolism in regulating fungal
826 morphogenesis. Our sulfur add-back experiments demonstrated that cysteine or
827 methionine rescued the morphogenetic defects exhibited by the *met32* knockout strain,
828 further solidifying the direct involvement of sulfur metabolism in this morphogenetic
829 switching process. How active sulfur metabolism contributes towards fungal
830 morphogenesis is not yet understood but given its critical requirement during this
831 phenomenon, it would be an important question to explore and will further our overall
832 understanding of this important biological phenomenon.
833
834 It is interesting to note that the expression of Met4, the principal transcriptional regulator
835 of the *de novo* biosynthesis of sulfur-containing amino acids in *S. cerevisiae* along with
836 Met32 one of its cognate DNA-binding cofactors (Blaiseau et al., 1997), are significantly
837 downregulated when glycolysis is perturbed. Given the obligate requirement of Met4
838 interaction with DNA-binding proteins such as Met28, Met32, or Met31, to elicit
839 transcriptional activation of the genes involved in the *de novo* biosynthesis of sulfur-
840 containing amino acids (Blaiseau and Thomas, 1998), the observed downregulation in both
841 Met4 and Met32 levels likely compromises the overall biosynthesis of sulfur-containing
842 amino acids. This concurrent downregulation could explain the attenuated expression of
843 downstream genes involved in the synthesis of methionine and cysteine. This suggests a
844 novel regulatory mechanism wherein the expression of Met4/Met32 is coupled to glycolytic
845 activity, under nitrogen-limiting conditions. Given that sulfur metabolism is coupled to

846 glycolysis in *C. albicans* as well and contributes towards fungal morphogenesis, it is likely
847 that this conserved regulatory axis might be critical for fungal morphogenesis in a broad
848 range of fungal species. Interestingly, Met4 regulation is directly dependent on Met30
849 (Rouillon et al., 2000). Met30 functions as a molecular switch for Met4, the master
850 regulator of the *MET* gene network. Under sulfur replete conditions, Met30 ensures that
851 Met4 remains inactive through ubiquitination and proteasomal degradation. Conversely, a
852 reduction in sulfur availability diminishes Met30 activity, thereby de-repressing Met4 and
853 allowing it to induce the expression of genes necessary for sulfur amino acid biosynthesis
854 (Rouillon et al., 2000; Smothers et al., 2000; Thomas and Surdin-Kerjan, 1997). Given
855 this regulatory mechanism, we investigated the expression of proteins involved in the
856 sulfur assimilation pathway (Met4, Met32, Met16 and Cys3), in a viable *Δmet30* deletion
857 strain, under conditions where glycolysis was perturbed using 2DG. We observed no
858 difference in protein levels of Met4, Met32, Met16 and Cys3, between 2DG treated and
859 untreated cells. This indicates that, in the heterozygous deletion strain of *met30* (*Δmet30*),
860 Met4 is not degraded even when glycolysis is perturbed, supporting the hypothesis that
861 perturbing active glycolysis with inhibitors like 2DG increases Met30 activity, which in turn
862 leads to the increased degradation of Met4, which would then negatively affect *MET* gene
863 transcription subsequently attenuating pseudohyphal differentiation. However, a
864 surprising finding emerged when we examined Met30 levels in the presence of 2DG. There
865 was no increase in the levels of Met30 in 2DG treated cells compared to untreated cells.
866 This suggests that glycolysis influences Met30 activity through a post-translational
867 mechanism, rather than by altering its protein abundance. Studies have shown that under
868 cadmium stress, Met4 activity is upregulated by reducing the activity of Met30 through
869 post-translational events, specifically by inducing the dissociation of Met30 from the core
870 SCF (Skp1/Cullin1/F-box) complex without affecting Met30 protein levels (Lauinger et al.,
871 2024; Yen et al., 2005). This well-established paradigm provides a compelling framework
872 for our observation, suggesting that active glycolytic flux, similar to cadmium stress, might
873 rapidly modulate the activity of Met30 by decreasing its association with the SCF complex
874 to control Met4 activity, rather than through changes in protein synthesis or degradation.
875 Future studies will be needed to delineate the precise post-translational modifications or
876 regulatory interactions that modulate Met30 activity in response to glycolytic flux.
877
878 Intriguingly, our work extended these findings to the pathogenic fungus *C. albicans*,
879 revealing a conserved role for glycolysis-mediated sulfur metabolism in hyphal
880 differentiation, a key virulence attribute in this species (Gow et al., 2012; Moyes et al.,
881 2016; Wilson et al., 2016). Similar to our observations in *S. cerevisiae*,
882 *C. albicans* exhibited glycolysis-dependent hyphal formation under nitrogen limitation in a
883 cAMP-PKA pathway independent manner. Perturbation of glycolysis (either by 2DG
884 addition or the deletion of *pfk1*) resulted in the significant downregulation of genes
885 involved in *de novo* biosynthesis of sulfur-containing amino acids (*met32*, *met3, met5*
886 (*ecm17*), *met10* and *met17* (*met15*)) and the hyphal differentiation defects that occur in
887 response to glycolysis perturbation could be rescued by the exogenous supplementation
888 of cysteine or methionine , wherein the exogenous addition of cAMP failed to rescue the
889 hyphal defects caused by the addition of 2DG. These results clearly demonstrate that *de*
890 *novo* biosynthesis of sulfur-containing amino acids is a critical downstream effector of
891 glycolytic activity in promoting hyphal differentiation under nitrogen-limiting conditions, in
892 *C. albicans* as well. Given that central carbon metabolic pathways like glycolysis and sulfur
893 assimilation pathway are broadly conserved metabolic processes across a plethora of
894 fungal species, it is possible that this novel regulatory axis might play a crucial role in
895 modulating fungal morphogenesis in multiple fungal species and further studies are

warranted to explore this. Finally, given the established link between hyphal differentiation and *C. albicans* virulence, we explored the impact of glycolytic perturbation on the pathogenicity of this fungus. Interestingly, RT-qPCR analysis revealed a significant downregulation of genes involved in hyphal differentiation and virulence (*als3, ece1, hwp1, hyr1, ihd1, rbt1* and *sap6*) upon 2DG treatment and in the *ΔΔpfk1* strain. Interestingly, deletions of sugar kinases or transcription factors regulating the expression of glycolysis genes or *adh1* in *C. albicans* leads to filamentation defects and downregulation of filamentation/virulence-specific genes (Askew et al., 2009; Laurian et al., 2019; Song et al., 2019). Our data, showing transcriptional downregulation of hyphal differentiation and virulence genes following glycolytic perturbation *via* the deletion of *pfk1*, strongly corroborate these previous findings. This collectively positions glycolysis as a central metabolic nexus, rather than merely a catabolic process, profoundly influencing the pathogenic ability of *C. albicans* by intricately linking cellular metabolism, morphogenetic transitions, and the expression of its virulence factors. Furthermore, the *ΔΔpfk1* strain displayed significantly reduced survival within *murine* macrophages and attenuated virulence in a *murine* model of systemic candidiasis, as evidenced by increased host survival, lower kidney fungal burden, and reduced tissue colonization. Remarkably, exogenous sulfur supplementation (N-acetyl cysteine (NAC)) to mice rescued the attenuated virulence exhibited by *ΔΔpfk1*. It is important to note that, in the context of certain bacterial pathogens, NAC has been reported to augment cellular respiration, subsequently increasing Reactive Oxygen Species (ROS) generation, which contributes to pathogen clearance (Shee et al., 2022). Interestingly, in our study, NAC supplementation to the mice was given prior to the infection and maintained continuously throughout the duration of the experiment. This continuous supply of NAC likely contributes to the rescue of virulence defects exhibited by the *ΔΔpfk1* strain. Essentially, NAC likely allows the mutant to fully activate its essential virulence strategies (including morphological switching), to cause a successful infection in the host. These findings underscore the critical role of glycolysis, and by extension, glycolysis-dependent sulfur metabolism, in the virulence of *C. albicans*.

In conclusion, our study unveils a conserved metabolic network that orchestrates fungal morphogenesis in response to nutrient availability. We demonstrate that active glycolysis, fueled by fermentable carbon sources in a cAMP-PKA independent manner, plays a crucial role in regulating the *de novo* biosynthesis of sulfur-containing amino acids in Met30-dependent manner, which in turn are essential for the morphological transitions in both *S. cerevisiae* and *C. albicans* (Fig. 6). The attenuation of *C. albicans* virulence upon disruption of this pathway highlights the potential of targeting specific fungal metabolic networks as a novel antifungal strategy. Future research in our laboratory will focus on elucidating the precise molecular mechanisms by which glycolytic intermediates or downstream signals regulate the expression of sulfur metabolism pathway and how sulfur-containing amino acids contribute to the cellular processes underlying fungal morphogenesis.

946 # Materials and Methods
947
948 **Yeast Strains:**
949 The prototrophic diploid strains, ∑1278b or CEN.PK were used in all the experiments
950 involving *S. cerevisiae*. The prototrophic diploid strain, SC5314 was exclusively used in all
951 the experiments involving *C. albicans*. The yeast strains used in this study are listed in
952 Suppl.Table 1.
953
954 **Generation of *S. cerevisiae* Gene Knockout and Epitope-tagged Strains:**
955 A standard PCR-based technique was used to amplify resistance cassettes (G418, HygB,
956 or NAT) with flanking sequences in order to carry out gene deletions. The target gene was
957 then replaced by homologous recombination using the lithium acetate-based
958 transformation (Schiestl and Gietz, 1989). Similarly, C-terminal epitope-tagged yeast
959 strains were generated using a PCR-based technique. This involved amplifying resistance
960 cassettes, flanked by sequences homologous to the C-terminal region of the target gene,
961 along with the desired epitope tags. The targeted gene was then tagged at its C-terminus
962 through homologous recombination, using the lithium acetate-based transformation
963 method. Primers used for these experiments are listed in Suppl.Table 2.
964
965 **Generation of *C. albicans* Gene Knockout Strains:**
966 The *C. albicans* strains used in this study are listed in Suppl.Table 1. The previously
967 established SAT1-flipper method was used with some modifications, for the deletion of the
968 desired gene (Reuß et al., 2004). To generate the *pfk1* deletion (*ΔΔpfk1*) strain, a DNA
969 fragment carrying the flanking regions of *pfk1* (100 bps homology) and the *SAT1*-flipper
970 cassette was transformed into *C. albicans* wild-type SC5314, using electroporation.
971 Transformants were selected based on their nourseothricin (NAT) resistance. PCR
972 confirmation was used to validate the transformants. The *SAT1*-flipper cassette was then
973 excised from the *pfk1* locus by growing the cells in YPM medium (10g/l yeast extract, 20g/l
974 peptone, and 2% (w/v) maltose) to induce expression of the *MAL2* promoter-regulated
975 recombinase. To knock out the second allele of *pfk1*, the heterozygous *pfk1* deletion
976 mutants (*Δpfk1/PFK1)* were used for the transformation wherein the DNA fragment
977 carrying the flanking regions of *pfk1* (100 bps homology) and the *SAT1*-flipper cassette
978 was transformed into *C. albicans Δpfk1/PFK1* SC5314. Transformants were selected based
979 on their NAT resistance. PCR confirmation was used to validate the transformants. Primers
980 used to generate or confirm the deletion strains are listed in Suppl.Table 2.
981
982 **Media and Growth Conditions:**
983 YPD broth containing 10g/l yeast extract, 20g/l peptone and 2% (w/v) glucose was used
984 for the overnight growth of the cultures. Nitrogen-limiting medium containing 1.7g/l yeast
985 nitrogen base without amino acids or ammonium sulfate, 2% (w/v) glucose (SLAD), 50μM
986 ammonium sulfate and 2% (w/v) agar which was extensively washed, to remove excess
987 nitrogen (Gimeno et al., 1992) was used for all experiments involving pseudohyphal or
988 hyphal differentiation. Overnight cultures of various strains were grown in YPD broth and
989 incubated at 30 °C with continuous shaking at 200 rotations per minute (RPM). Reagents
990 and tools used in this study are mentioned in Suppl.Table 3.
991
992 **Pseudohyphal Differentiation Assay:**
993 To induce pseudohyphal differentiation in *S. cerevisiae,* overnight cultures of various
994 strains (listed in Suppl.Table 1) were spotted on nitrogen-limiting medium (SLA)

containing 2% (w/v) glucose (SLAD). In order to check the effect of glycolysis inhibitors, 0.05% (w/v) concentration of 2-Deoxy-D-Glucose (2DG) and 0.2% (w/v) concentration of sodium citrate (NaCi), on pseudohyphal differentiation, wild-type was spotted on SLAD containing sub-inhibitory concentrations of 2DG (0.05% w/v) or NaCi (0.2% w/v). Plates were incubated for 10 days at 30 °C (Chandarlapaty and Errede, 1998; González et al., 2017). After 10 days, imaging was done using Olympus MVX10 stereo microscope. Cells from colonies were isolated and single cells were imaged using Zeiss Apotome microscope. Length/width ratio of individual cells was measured using ImageJ and percentage of pseudohyphal cells from total population was determined. Cells with a length/width ratio of 2 or more were considered as pseudohyphal cells as described previously (Schröder et al., 2000). Statistical analysis was done using unpaired t-test or one-way ANOVA test. Error bars represent SEM. All the experiments were performed independently, thrice.

Hyphal Differentiation Assay:

To induce hyphal differentiation in *C. albicans,* overnight cultures of each strain (listed in Suppl.Table 1) were spotted on nitrogen-limiting medium (SLAD). To check the effect of glycolysis inhibitor, 2DG on hyphal differentiation, wild-type was spotted on SLAD containing sub-inhibitory concentration of 2DG (0.2% w/v). All the plates were incubated for 7 days at 37 °C (Sánchez-Martínez and Pérez-Martín, 2002; Song et al., 2019). After 7 days, cells from colonies were isolated and single cells were imaged using Zeiss Apotome microscope. Length/width ratio of individual cells was measured using ImageJ and percentage of hyphal cells from total population was determined. Cells with a length/width ratio of 4.5 or more were considered as hyphal cells as described previously (Su et al., 2018). Statistical analysis was done using unpaired t-test or one-way ANOVA test. Error bars represent SEM. All the experiments were performed independently, thrice.

Growth Curves:

Growth curve analysis in the presence of glycolysis inhibitors (2DG or NaCi) was performed as follows. Overnight grown cultures of wild-type strains (∑1278b or CEN.PK or SC5314) were diluted to OD_{600}=0.01 in fresh SLAD medium with and without 2DG or NaCi and allowed to grow at 30 °C for 24 hours. OD_{600} was recorded at 3-h intervals. Growth curve analysis using various deletion strains were performed as follows. Overnight grown cultures of various deletion strains (listed in Suppl.Table 1) along with wild-type strains (∑1278b or CEN.PK or SC5314) were diluted to OD_{600}=0.01 in fresh SLAD and allowed to grow at 30 °C for 24 hours. OD_{600} was recorded at 3-h intervals. Graphs were prepared using GraphPad Prism. Error bars represent SEM. All the experiments were performed independently, thrice.

cAMP Add-back Assays:

In order to perform cAMP add-back assays, overnight cultures of wild-type ∑1278b and various deletion strains of *S. cerevisiae* (listed in Suppl.Table 1) were spotted on SLAD or SLAD containing sub-inhibitory concentration of 2DG or NaCi, in the presence and absence of cAMP (1mM) (Lorenz, 1997). Plates were incubated for 10 days at 30 °C. After 10 days, imaging was done using Olympus MVX10 stereo microscope. Cells from colonies were isolated and single cells were imaged using Zeiss Apotome microscope. Length/width ratio of individual cells was measured using ImageJ and percentage of pseudohyphal cells from total population was determined. For hyphal differentiation assays in *C. albicans*, overnight cultures of wild-type SC5314 and *ΔΔpfk1* strains of *C. albicans* were spotted on SLAD or SLAD containing sub-inhibitory concentration of 2DG, in the presence and absence of cAMP (5mM) (Li et al., 2013). Plates were incubated for 7 days at 37 °C. After 7 days, cells from

colonies were isolated and single cells were imaged using Zeiss Apotome microscope. Length/width ratio of individual cells was measured using ImageJ and percentage of hyphal cells from total population was determined. Statistical analysis was done using one-way ANOVA test. Error bars represent SEM. All the experiments were performed independently, thrice.

Sulfur Add-back Assays:

In order to perform sulfur add-back assays, overnight cultures of various strains of *S. cerevisiae* or *C. albicans* (listed in Suppl.Table 1) were spotted on SLAD or SLAD containing sub-inhibitory concentration of 2DG, in the presence and absence of sulfur-containing compounds including cysteine, methionine. Plates were incubated for 10 days at 30 °C to induce pseudohyphal differentiation in *S. cerevisiae*. After 10 days, imaging was done using Olympus MVX10 stereo microscope. Cells from colonies were isolated and single cells were imaged using Zeiss Apotome microscope. Length/width ratio of individual cells was measured using ImageJ and percentage of pseudohyphal cells from total population was determined. For hyphal differentiation assays in *C. albicans*, plates were incubated for 7 days at 37 °C. After 7 days, cells from colonies were isolated and single cells were imaged using Zeiss Apotome microscope. Length/width ratio of individual cells was measured using ImageJ and percentage of hyphal cells from total population was determined. Statistical analysis was done using unpaired t-test or one-way ANOVA test. Error bars represent SEM. All the experiments were performed independently, thrice.

Whole genome sequencing:

Sample Collection. Strains of *S. cerevisiae* (*ΔΔpfk1* or *ΔΔadh1* along with wild-type strain ∑1278b) or *C. albicans* (*ΔΔpfk1* along with wild-type strain SC5314) were grown in YPD medium at 30 °C for overnight.

Genomic DNA Extraction. Genomic DNA from the samples was extracted using phenol-chloroform method. Following RNAse treatment to eliminate any contaminating RNA from the sample, the extracted DNA was submitted to the CCMB next-generation sequencing facility for whole genome sequencing.

Whole genome sequencing Analysis. Raw sequencing reads were obtained in FASTQ format. The reference genome and annotation files for the *S. cerevisiae* strain ∑1278b were downloaded from the Saccharomyces Genome Database (SGD) and reference genome and annotation files for the *C. albicans* strain SC5314 were downloaded from the NCBI (National Center for Biotechnology Information). Quality assessment of the raw reads was performed using FastQC (version 0.12.1). Adapter sequences were trimmed using Cutadapt (version 4.6). The reference genome was indexed with Hisat2 (version 2.2.1), and Samtools (version 1.20) was used to filter out multi-mapped reads and convert SAM files to BAM format. Visualisation of reads was done using IGV software (version 2.16.2).

RNA-Sequencing:

Sample Collection. Overnight culture of *S. cereviae* wild-type ∑1278b was spotted on nitrogen-limiting media containing 2% (w/v) glucose (SLAD) with and without sub-inhibitory concentration of 2DG. The plates were incubated at 30 °C and colonies were isolated on day 5 (D-5) and day 10 (D-10).

1094 **RNA-Extraction.** Total RNA from the sample was extracted using the protocol mentioned
1095 in the Ribopure RNA purification kit (yeast) (cat. #AM1926). Following a DNAse treatment
1096 to eliminate any genomic DNA from the sample, the extracted RNA was submitted to the
1097 CCMB next-generation sequencing facility for RNA-Seqencing. The NovaSeq 6000
1098 equipment was used to sequence transcriptomes.
1099
1100 **RNA-Sequencing Analysis.** Raw sequencing reads were obtained in FASTQ format. The
1101 reference genome and annotation files for the *S. cerevisiae* strain ∑1278b were
1102 downloaded from the Saccharomyces Genome Database (SGD). Quality assessment of the
1103 raw reads was performed using FastQC (version 0.12.1). Adapter sequences were trimmed
1104 using Cutadapt (version 4.6). The reference genome was indexed with Hisat2 (version
1105 2.2.1), and Samtools (version 1.20) was used to filter out multi-mapped reads and convert
1106 SAM files to BAM format. Read counting for uniquely mapped reads was done with
1107 FeatureCounts, using gene annotation data from the reference *S. cerevisiae* ∑1278b
1108 genome. Normalization and differential gene expression analysis were performed using
1109 R (version 4.3.2). Genes with a $\log_2$ fold change of ≥1 were considered to be upregulated,
1110 indicating at least a doubling in expression under the given condition, while those with a
1111 $\log_2$ fold change of ≤ -1 were considered to be downregulated.
1112
1113 **Protein Isolation:**
1114 For Western blotting experiments, in order to isolate proteins from liquid cultures,
1115 overnight yeast cultures were back-diluted in 10 ml of liquid SLAD in the presence and
1116 absence of 2DG. The yeast cells were grown till an OD_{600} of ~1 and cells were harvested
1117 by centrifugation at 3000 rpm for 10 minutes at room temperature (RT). To isolate proteins
1118 from colonies, overnight cultures of pertinent strains were spotted on SLAD with and
1119 without sub-inhibitory concentration of 2DG (0.05% (w/v)) and colonies were isolated and
1120 resuspended in 1ml of 1X PBS (Phosphate Buffered Saline) after 5 days (D-5). Cells were
1121 harvested by centrifugation at 14000 rpm for 10 minutes at room temperature. Pelleted
1122 cells (from liquid cultures and colonies) were resuspended in 300µl of ice cold 10% (w/v)
1123 TCA solution and disrupted using bead-beating by addition of 150µl of glass beads at 4°C.
1124 Supernatant was transferred to another tube. Next, proteins were pelleted by
1125 centrifugation at 14,000 rpm for 10 minutes at 4 °C and supernatant was discarded. Each
1126 pellet was resuspended in 400µl of SDS/glycerol buffer (7.3% (w/v) SDS, 29% (v/v)
1127 glycerol and 83.3mM tris-base) and boiled at 95 °C for 10 minutes with occasional
1128 vortexing followed by centrifugation at 14,000 rpm for 10 minutes at room temperature.
1129 Supernatant was transferred to a fresh tube and used for protein estimation using BCA
1130 protein estimation kit (cat. #23227). Finally, all samples were diluted in SDS-PAGE loading
1131 buffer (100mM Tris-Cl, 4% (w/v) SDS, 0.02% (w/v) bromophenol blue, 20% (w/v),
1132 glycerol and 7.5% (v/v) β-mercaptoethanol) and heated for 5 minutes at 90 °C.
1133
1134 **Immunodetection:**
1135 Protein samples were separated using SDS-PAGE on polyacrylamide gels and transferred
1136 to PVDF membranes with a Mini Trans-Blot Cell module (Bio-Rad). The membranes were
1137 blocked for 1 hour at room temperature with 5% (w/v) non-fat dry milk in 1X TBST buffer
1138 (20mM Tris-Base, pH 7.6, 150mM NaCl, 0.1% (v/v) Tween-20) with gentle orbital shaking.
1139 After blocking, the membranes were incubated overnight at 4°C with primary antibodies
1140 (1:2000 dilution) in 1X TBST buffer containing 5% (w/v) non-fat dry milk. Following this,
1141 the membranes were washed three times for 10 minutes in 1X TBST and then incubated
1142 for 1 hour at room temperature with HRP-conjugated secondary antibodies (1:4000
1143 dilution) in 1X TBST with 5% (w/v) non-fat dry milk. After three additional washes in 1X

1144 TBST, chemiluminescent substrate was added and bands were detected using the
1145 SuperSignal West chemiluminescent substrate (cat. #34579, cat. #34094) and visualized
1146 using the Bio-Rad ChemiDoc™ MP imaging system.
1147
1148 **Antibodies:**
1149 HA-Tag (C29F4) Rabbit mAb (cat. #3724), β-actin (8H10D10) Mouse mAb (cat. #3700),
1150 Goat anti-Rabbit IgG-HRP conjugate (cat. #7074) and Horse anti-Mouse IgG-HRP
1151 conjugate (cat. #7076) were purchased from Cell Signaling Technology. Pgk1 Mouse mAb
1152 (cat. #sc-130335) was purchased from Santa Cruz Biotechnology.
1153
1154 **Densitometric Analysis:**
1155 Raw images of Western blots were analysed using ImageJ to normalize target protein
1156 expression with the expression of housekeeping proteins including PGK1 or β-actin in order
1157 to make densitometric graphs. Statistical analysis was done using unpaired t-test, with
1158 error bars representing SEM. All the experiments were performed independently, thrice.
1159
1160 **Quantitative Real Time Polymerase Chain Reaction (RT-qPCR) Assay:**
1161 For *S. cerevisiae*, overnight cultures of *ΔΔpfk1* and *ΔΔadh1* along with wild-type strain
1162 ∑1278b were spotted on SLAD and plates were incubated at 30 °C for ~4 days. After 4
1163 days, colonies were isolated and total RNA was extracted using the protocol mentioned in
1164 the Ribopure RNA purification kit, yeast (cat. #AM1926). cDNA synthesis was carried out
1165 using PrimeScript cDNA synthesis kit (cat. #6110A). Primers used for RT-qPCR were
1166 designed using PrimeQuest tool of Integrated DNA Technologies (IDT). RT-qPCR was
1167 performed using iTaq Universal SYBR green mastermix (cat. #1725121). Actin was used
1168 as housekeeping gene for normalization. The results were analysed using the $2^{-\Delta\Delta CT}$ method
1169 (Winer et al., 1999) and statistical analysis was done using one-way ANOVA test, with
1170 error bars representing SEM. All the experiments were performed independently, thrice.
1171 Primers used in the RT-qPCR experiments are mentioned in Suppl.Table 2.
1172
1173 For *C. albicans*, overnight cultures of *C. albicans* wild-type SC5314 was spotted on SLAD
1174 with and without sub-inhibitory concentration of 2DG (0.2% w/v) or *C. albicans ΔΔpfk1*
1175 strain along with wild-type SC5314 was spotted on SLAD and plates were incubated at
1176 37 °C for 4 days. After 4 days, colonies were isolated and total RNA was extracted using
1177 the protocol mentioned in the Ribopure RNA purification kit, yeast (cat. #AM1926). cDNA
1178 synthesis was carried out using PrimeScript cDNA synthesis kit (cat. #6110A). Primers
1179 used for RT-qPCR were designed using PrimeQuest tool of Integrated DNA Technologies
1180 (IDT). RT-qPCR was performed using iTaq Universal SYBR green mastermix (cat.
1181 #1725121). Actin was used as housekeeping gene for normalization. The results were
1182 analysed using the $2^{-\Delta\Delta CT}$ method (Winer et al., 1999) and statistical analysis was done
1183 using one-way ANOVA test, with error bars representing SEM. All the experiments were
1184 performed independently, thrice. Primers used in the RT-qPCR experiments are mentioned
1185 in Suppl.Table 2.
1186
1187 ***In vitro* Microbial Survival Assay:**
1188 *In vitro* microbial survival assay in macrophages was conducted as described in previous
1189 studies with some modifications (Netea et al., 2002; Pradhan et al., 2016). *RAW 264.7*
1190 macrophages (1×10^6 cells) were cultured in six-well plates with DMEM supplemented with
1191 10% FBS. After 16 hours of incubation, the cells were treated with *C. albicans* wild-type
1192 SC5314 or *ΔΔpfk1* at a multiplicity of infection (MOI) of 10, for 1 hour in antibiotic-free
1193 DMEM containing 10% FBS. The media was then removed, and the cells were washed six

1194 times with 1X PBS to eliminate any free, non-phagocytosed fungal cells. Next, the cells
1195 were lysed with 350 µl of lysis buffer containing 0.025% SDS in 1X PBS. The lysate volume
1196 was adjusted to 1 ml with 1X PBS, and a 100 µl undiluted aliquot was plated on YPD agar
1197 plate. Serial dilutions of the lysate were also plated on YPD agar plates. These plates were
1198 incubated overnight at 37 °C. The following day, colony forming units (CFU) were counted
1199 and plotted. The percentage of survival was calculated as the number of CFU in the
1200 presence of macrophages divided by the number of CFU in the absence of macrophages.
1201 Statistical analysis was done using unpaired t-test, with error bars representing SEM. All
1202 the experiments were performed independently, thrice.
1203
1204 ***In vivo Murine* Model of Systemic Candidiasis:**
1205 *In vivo* infection experiments were performed as previously described (Majer et al., 2012).
1206 Briefly, *C. albicans* wild-type SC5314 and *ΔΔpfk1* were grown overnight in YPD medium
1207 at 30 °C. The overnight cultures were back-diluted in 10 ml of YPD liquid medium and
1208 allowed to grow till OD of ~0.6, then washed and resuspended in 1X PBS. C57BL/6 wild-
1209 type mice, aged 6 to 8 weeks, were injected intravenously *via* lateral tail vein with
1210 *C. albicans* wild-type SC5314 (1×10^7 CFU) or *ΔΔpfk1* (1×10^7 CFU). After infection, mice
1211 were monitored for survival and daily for signs of morbidity and mortality were recorded
1212 over a period of 21 days. Survival data were analysed using the Log-rank Mantel-Cox test.
1213 In order to perform *in vivo* sulfur supplementation, N-acetyl cysteine (NAC) was dissolved
1214 in distilled water at a concentration of 6mg/ml and administrated orally to mice before 72
1215 hours of *C. albicans* infection. Normal distilled water administration to mice was used as
1216 control. After 72 hours of NAC administration, C57BL/6 wild-type mice, aged 6 to 8 weeks,
1217 were infected with SC5314 (1×10^7 CFU) or *ΔΔpfk1* strain (1×10^7 CFU), intravenously
1218 *via* lateral tail vein injection. After infection, mice were monitored for survival and daily
1219 for signs of morbidity and mortality were recorded over a period of 21 days. Survival data
1220 were analysed using the Log-rank Mantel-Cox test.
1221
1222 **Determination of Fungal Burden:**
1223 To assess fungal burden, mice injected with *C. albicans* wild-type SC5314 or *ΔΔpfk1* were
1224 sacrificed at ~2 days and kidneys were harvested from infected mice. Kidneys were
1225 weighed and then homogenized using a sterilized and 1X PBS-washed Dounce
1226 homogenizer (cat. #D8938). Kidney suspensions were then diluted in 1 ml of 1X PBS and
1227 serially diluted. Then 100µl of dilutions was plated on YPD agar plates and allowed to grow
1228 at 37 °C. Colony forming units (CFU) were calculated by the following formula: (number
1229 of colonies × dilution factor × 10)/organ weight in grams (g). Statistical analysis was done
1230 using unpaired t-test. Error bars represent SEM. All the experiments were performed
1231 independently, thrice.
1232
1233 **Histopathology:**
1234 For histopathological examination, kidneys were collected and fixed in 10% neutral
1235 buffered formalin for about two weeks. After fixation, the kidneys were processed,
1236 embedded in paraffin, and sectioned to 4µm thickness. The tissue sections were then
1237 stained using the GMS stain (Grocott Methenamine Silver stain) as per the manufacturer's
1238 protocol (cat. #AB287884).
1239
1240 **Illustrations:**
1241 Figure illustrations were created using Biorender (https://app.biorender.com).
1242
1243

Animal Ethics Statement:

All animal experiments in this manuscript were reviewed and approved by the Institutional Animal Ethics Committee (IAEC) of CSIR-Centre for Cellular and Molecular Biology (Approval number: 52/2024-C).

Data Availability:

All relevant data are within the paper and its supporting information files, except for RNA-Seq data and Whole Genome Sequencing data. RNA-Seq data and Whole Genome Sequencing data are deposited in NCBI's SRA database and are accessible through BioProject accession number PRJNA1263201. (https://www.ncbi.nlm.nih.gov/bioproject/PRJNA1263201)

Acknowledgements

We thank Dr. Rajan Sankaranarayanan (CSIR-CCMB) and Dr. Sunil Laxman (BRIC-InStem) for critical reading of our manuscript. We gratefully acknowledge the invaluable support and resources offered by CSIR-Centre for Cellular and Molecular Biology (CCMB) central facilities including Advanced Microscopy and Imaging facility (AMIF), Next Generation Sequencing (NGS) facility and Animal House facility. We acknowledge help from T. Avinash Raj (CSIR- CCMB) for preparation of samples for histological analysis. DS thanks University Grants Commission (UGC), India for their research fellowship. SV acknowledges funding from Indian Council of Medical Research (ICMR) (IIRPSG-2024-01-02717), India; Anusandhan National Research Foundation (ANRF) (SRG/2023/000470), India; Council of Scientific & Industrial Research (CSIR) (FTT070505), India; and DBT-Wellcome Trust India Alliance (IA/E/16/1/502996), India.

Author Contributions

Dhrumi Shah: Conceptualization; Investigation; Formal analysis; Visualization; Writing-original draft. **Nikita Rewatkar:** Investigation. **Adishree M:** Investigation. **Siddhi Gupta:** Investigation. **Sudharsan Mathivathanan:** Investigation. **Sayantani Biswas:** Investigation. **Sriram Varahan:** Conceptualization; Supervision; Funding acquisition; Investigation; Formal analysis; Visualization; Writing-original draft; Writing-review and editing.

Conflict of Interest

The authors declare that they have no conflict of interests.

References

1. Askew, C., Sellam, A., Epp, E., Hogues, H., Mullick, A., Nantel, A., & Whiteway, M. (2009). Transcriptional regulation of carbohydrate metabolism in the human pathogen Candida albicans. *PLoS pathogens*, *5*(10), e1000612. https://doi.org/10.1371/journal.ppat.1000612
2. Bailey, D. A., Feldmann, P. J., Bovey, M., Gow, N. A., & Brown, A. J. (1996). The Candida albicans HYR1 gene, which is activated in response to hyphal development, belongs to a gene family encoding yeast cell wall proteins. Journal of bacteriology, 178(18), 5353–5360. https://doi.org/10.1128/jb.178.18.5353-5360.1996
3. Barford JP, Hall RJ. 1979. An examination of the crabtree effect in Saccharomyces cerevisiae: The role of respiratory adaptation. J Gen Microbiol. https://doi.org/10.1099/00221287-114-2-267
4. Bennetzen, J. L., & Hall, B. D. (1982). The primary structure of the Saccharomyces cerevisiae gene for alcohol dehydrogenase. The Journal of biological chemistry, 257(6), 3018–3025. https://doi.org/10.1016/S0021-9258(19)81067-0
5. Biswas, S., Van Dijck, P., & Datta, A. (2007). Environmental sensing and signal transduction pathways regulating morphopathogenic determinants of Candida albicans. Microbiology and molecular biology reviews : MMBR, 71(2), 348–376. https://doi.org/10.1128/MMBR.00009-06
6. Blaiseau, P. L., & Thomas, D. (1998). Multiple transcriptional activation complexes tether the yeast activator Met4 to DNA. The EMBO journal, 17(21), 6327–6336. https://doi.org/10.1093/emboj/17.21.6327
7. Blaiseau, P. L., Isnard, A. D., Surdin-Kerjan, Y., & Thomas, D. (1997). Met31p and Met32p, two related zinc finger proteins, are involved in transcriptional regulation of yeast sulfur amino acid metabolism. Molecular and cellular biology, 17(7), 3640–3648. https://doi.org/10.1128/MCB.17.7.3640
8. Broach J. R. (2012). Nutritional control of growth and development in yeast. Genetics, 192(1), 73–105. https://doi.org/10.1534/genetics.111.135731
9. Chandarlapaty, S., & Errede, B. (1998). Ash1, a daughter cell-specific protein, is required for pseudohyphal growth of Saccharomyces cerevisiae. Molecular and cellular biology, 18(5), 2884–2891. https://doi.org/10.1128/MCB.18.5.2884
10. Chebaro, Y., Lorenz, M., Fa, A., Zheng, R., & Gustin, M. (2017). Adaptation of Candida albicans to Reactive Sulfur Species. Genetics, 206(1), 151–162. https://doi.org/10.1534/genetics.116.199679
11. Christensen, M. (1989). A View of Fungal Ecology. Mycologia, 81(1), 1–19. https://doi.org/10.1080/00275514.1989.12025620
12. Christopher Thomas Evans and Colin Ratledge. 1985. Partial purification and properties of pyruvate kinase and its regulatory role during lipid accumulation by the oleaginous yeast Rhodosporidium toruloides CBS 14. Canadian Journal of Microbiology. 31(5): 479-484. https://doi.org/10.1139/m85-089
13. Colombo, S., Ma, P., Cauwenberg, L., Winderickx, J., Crauwels, M., Teunissen, A., Nauwelaers, D., de Winde, J. H., Gorwa, M. F., Colavizza, D., & Thevelein, J. M. (1998). Involvement of distinct G-proteins, Gpa2 and Ras, in glucose- and intracellular acidification-induced cAMP signalling in the yeast Saccharomyces cerevisiae. The EMBO journal, 17(12), 3326–3341. https://doi.org/10.1093/emboj/17.12.3326
14. Csank, C., Schröppel, K., Leberer, E., Harcus, D., Mohamed, O., Meloche, S., Thomas, D. Y., & Whiteway, M. (1998). Roles of the Candida albicans mitogen-activated protein kinase homolog, Cek1p, in hyphal development and systemic candidiasis. Infection and immunity, 66(6), 2713–2721. https://doi.org/10.1128/IAI.66.6.2713-2721.1998
15. De Deken R. H. (1966). The Crabtree effect: a regulatory system in yeast. Journal of general microbiology, 44(2), 149–156. https://doi.org/10.1099/00221287-44-2-149
16. Deorukhkar SC, Roushani S (2017) Virulence Traits Contributing to Pathogenicity of Candida Species. J Microbiol Exp 5(1): 00140. https://doi.org/10.15406/jmen.2017.05.00140
17. Dickinson, J. R., Salgado, L. E., & Hewlins, M. J. (2003). The catabolism of amino acids to long chain and complex alcohols in Saccharomyces cerevisiae. The Journal of biological chemistry, 278(10), 8028–8034. https://doi.org/10.1074/jbc.M211914200

18. Dikicioglu, D., Karabekmez, E., Rash, B., Pir, P., Kirdar, B., & Oliver, S. G. (2011). How yeast re-programmes its transcriptional profile in response to different nutrient impulses. BMC systems biology, 5, 148. https://doi.org/10.1186/1752-0509-5-148
19. Düring-Olsen, L., Regenberg, B., Gjermansen, C., Kielland-Brandt, M. C., & Hansen, J. (1999). Cysteine uptake by Saccharomyces cerevisiae is accomplished by multiple permeases. Current genetics, 35(6), 609–617. https://doi.org/10.1007/s002940050459
20. Fleck, C. B., Schöbel, F., & Brock, M. (2011). Nutrient acquisition by pathogenic fungi: nutrient availability, pathway regulation, and differences in substrate utilization. International journal of medical microbiology : IJMM, 301(5), 400–407. https://doi.org/10.1016/j.ijmm.2011.04.007
21. Foy, J. J., & Bhattacharjee, J. K. (1978). Biosynthesis and regulation of fructose-1,6-bisphosphatase and phosphofructokinase in Saccharomyces cerevisiae grown in the presence of glucose and gluconeogenic carbon sources. Journal of bacteriology, 136(2), 647–656. https://doi.org/10.1128/jb.136.2.647-656.1978
22. Francis B. Cramer, Gladys E. Woodward, 2-Desoxy-D-glucose as an antagonist of glucose in yeast fermentation, Journal of the Franklin Institute, Volume 253, Issue 4, 1952, Pages 354-360, ISSN 0016-0032, https://doi.org/10.1016/0016-0032(52)90852-1
23. Gancedo J. M. (2001). Control of pseudohyphae formation in Saccharomyces cerevisiae. FEMS microbiology reviews, 25(1), 107–123. https://doi.org/10.1111/j.1574-6976.2001.tb00573.x
24. Gimeno, C. J., Ljungdahl, P. O., Styles, C. A., & Fink, G. R. (1992). Unipolar cell divisions in the yeast S. cerevisiae lead to filamentous growth: regulation by starvation and RAS. Cell, 68(6), 1077–1090. https://doi.org/10.1016/0092-8674(92)90079-r
25. González, B., Mas, A., Beltran, G., Cullen, P. J., & Torija, M. J. (2017). Role of Mitochondrial Retrograde Pathway in Regulating Ethanol-Inducible Filamentous Growth in Yeast. Frontiers in physiology, 8, 148. https://doi.org/10.3389/fphys.2017.00148
26. Gow, N. A., Brown, A. J., & Odds, F. C. (2002). Fungal morphogenesis and host invasion. Current opinion in microbiology, 5(4), 366–371. https://doi.org/10.1016/s1369-5274(02)00338-7
27. Gow, N. A., van de Veerdonk, F. L., Brown, A. J., & Netea, M. G. (2011). Candida albicans morphogenesis and host defence: discriminating invasion from colonization. Nature reviews. Microbiology, 10(2), 112–122. https://doi.org/10.1038/nrmicro2711
28. Harashima, T., & Heitman, J. (2002). The Galpha protein Gpa2 controls yeast differentiation by interacting with kelch repeat proteins that mimic Gbeta subunits. Molecular cell, 10(1), 163–173. https://doi.org/10.1016/s1097-2765(02)00569-5
29. Heinisch J. (1986). Construction and physiological characterization of mutants disrupted in the phosphofructokinase genes of Saccharomyces cerevisiae. Current genetics, 11(3), 227–234. https://doi.org/10.1007/BF00420611
30. Hirayama, T., Miyazaki, T., Ito, Y., Wakayama, M., Shibuya, K., Yamashita, K., Takazono, T., Saijo, T., Shimamura, S., Yamamoto, K., Imamura, Y., Izumikawa, K., Yanagihara, K., Kohno, S., & Mukae, H. (2020). Virulence assessment of six major pathogenic Candida species in the mouse model of invasive candidiasis caused by fungal translocation. Scientific reports, 10(1), 3814. https://doi.org/10.1038/s41598-020-60792-y
31. Huang G. (2012). Regulation of phenotypic transitions in the fungal pathogen Candida albicans. Virulence, 3(3), 251–261. https://doi.org/10.4161/viru.20010
32. Huang, C. W., Walker, M. E., Fedrizzi, B., Gardner, R. C., & Jiranek, V. (2017). Yeast genes involved in regulating cysteine uptake affect production of hydrogen sulfide from cysteine during fermentation. FEMS yeast research, 17(5), 10.1093/femsyr/fox046. https://doi.org/10.1093/femsyr/fox046
33. Jiménez-López, C., & Lorenz, M. C. (2013). Fungal immune evasion in a model host-pathogen interaction: Candida albicans versus macrophages. PLoS pathogens, 9(11), e1003741. https://doi.org/10.1371/journal.ppat.1003741
34. Kaiser, P., Sia, R. A., Bardes, E. G., Lew, D. J., & Reed, S. I. (1998). Cdc34 and the F-box protein Met30 are required for degradation of the Cdk-inhibitory kinase Swe1. Genes & development, 12(16), 2587–2597. https://doi.org/10.1101/gad.12.16.2587
35. Kosugi, A., Koizumi, Y., Yanagida, F., & Udaka, S. (2001). MUP1, high affinity methionine permease, is involved in cysteine uptake by Saccharomyces cerevisiae. Bioscience, biotechnology, and biochemistry, 65(3), 728–731. https://doi.org/10.1271/bbb.65.728

36. Kraakman, L., Lemaire, K., Ma, P., Teunissen, A. W., Donaton, M. C., Van Dijck, P., Winderickx, J., de Winde, J. H., & Thevelein, J. M. (1999). A Saccharomyces cerevisiae G-protein coupled receptor, Gpr1, is specifically required for glucose activation of the cAMP pathway during the transition to growth on glucose. Molecular microbiology, 32(5), 1002–1012. https://doi.org/10.1046/j.1365-2958.1999.01413.x
37. Kumar A. (2021). The Complex Genetic Basis and Multilayered Regulatory Control of Yeast Pseudohyphal Growth. Annual review of genetics, 55, 1–21. https://doi.org/10.1146/annurev-genet-071719-020249
38. Lauinger, L., Andronicos, A., Flick, K., Yu, C., Durairaj, G., Huang, L., & Kaiser, P. (2024). Cadmium binding by the F-box domain induces p97-mediated SCF complex disassembly to activate stress response programs. Nature communications, 15(1), 3894. https://doi.org/10.1038/s41467-024-48184-6
39. Laurian, R., Dementhon, K., Doumèche, B., Soulard, A., Noel, T., Lemaire, M., & Cotton, P. (2019). Hexokinase and Glucokinases Are Essential for Fitness and Virulence in the Pathogenic Yeast Candida albicans. Frontiers in microbiology, 10, 327. https://doi.org/10.3389/fmicb.2019.00327
40. Laxman, S., & Tu, B. P. (2011). Multiple TORC1-associated proteins regulate nitrogen starvation-dependent cellular differentiation in Saccharomyces cerevisiae. PloS one, 6(10), e26081. https://doi.org/10.1371/journal.pone.0026081
41. Li, D. D., Wang, Y., Dai, B. D., Li, X. X., Zhao, L. X., Cao, Y. B., Yan, L., & Jiang, Y. Y. (2013). ECM17-dependent methionine/cysteine biosynthesis contributes to biofilm formation in Candida albicans. Fungal genetics and biology : FG & B, 51, 50–59. https://doi.org/10.1016/j.fgb.2012.11.010
42. Lin, X., Alspaugh, J. A., Liu, H., & Harris, S. (2014). Fungal morphogenesis. Cold Spring Harbor perspectives in medicine, 5(2), a019679. https://doi.org/10.1101/cshperspect.a019679
43. Lionakis, M. S., Lim, J. K., Lee, C. C., & Murphy, P. M. (2011). Organ-specific innate immune responses in a mouse model of invasive candidiasis. Journal of innate immunity, 3(2), 180–199. https://doi.org/10.1159/000321157
44. Liu, Y., & Filler, S. G. (2011). Candida albicans Als3, a multifunctional adhesin and invasin. Eukaryotic cell, 10(2), 168–173. https://doi.org/10.1128/EC.00279-10
45. Lobo, Z., & Maitra, P. K. (1983). Phosphofructokinase mutants of yeast. Biochemistry and genetics. The Journal of biological chemistry, 258(3), 1444–1449. https://doi.org/10.1016/S0021-9258(18)33006-0
46. Lorenz, M. C., & Heitman, J. (1997). Yeast pseudohyphal growth is regulated by GPA2, a G protein alpha homolog. The EMBO journal, 16(23), 7008–7018. https://doi.org/10.1093/emboj/16.23.7008
47. Lorenz, M. C., & Heitman, J. (1998). Regulators of pseudohyphal differentiation in Saccharomyces cerevisiae identified through multicopy suppressor analysis in ammonium permease mutant strains. Genetics, 150(4), 1443–1457. https://doi.org/10.1093/genetics/150.4.1443
48. Lorenz, M. C., Pan, X., Harashima, T., Cardenas, M. E., Xue, Y., Hirsch, J. P., & Heitman, J. (2000). The G protein-coupled receptor gpr1 is a nutrient sensor that regulates pseudohyphal differentiation in Saccharomyces cerevisiae. Genetics, 154(2), 609–622. https://doi.org/10.1093/genetics/154.2.609
49. Maidan, M. M., De Rop, L., Serneels, J., Exler, S., Rupp, S., Tournu, H., Thevelein, J. M., & Van Dijck, P. (2005). The G protein-coupled receptor Gpr1 and the Galpha protein Gpa2 act through the cAMP-protein kinase A pathway to induce morphogenesis in Candida albicans. Molecular biology of the cell, 16(4), 1971–1986. https://doi.org/10.1091/mbc.e04-09-0780
50. Majer, O., Bourgeois, C., Zwolanek, F., Lassnig, C., Kerjaschki, D., Mack, M., Müller, M., & Kuchler, K. (2012). Type I interferons promote fatal immunopathology by regulating inflammatory monocytes and neutrophils during Candida infections. PLoS pathogens, 8(7), e1002811. https://doi.org/10.1371/journal.ppat.1002811
51. Martíez-Force, E., & Benítez, T. (1992). Changes in yeast amino acid pool with respiratory versus fermentative metabolism. Biotechnology and bioengineering, 40(6), 643–649. https://doi.org/10.1002/bit.260400602
52. Martin, R., Albrecht-Eckardt, D., Brunke, S., Hube, B., Hünniger, K., & Kurzai, O. (2013). A core filamentation response network in Candida albicans is restricted to eight genes. PloS one, 8(3), e58613. https://doi.org/10.1371/journal.pone.0058613

53. Masselot, M., & De Robichon-Szulmajster, H. (1975). Methionine biosynthesis in Saccharomyces cerevisiae. I. Genetical analysis of auxotrophic mutants. Molecular & general genetics : MGG, 139(2), 121–132. https://doi.org/10.1007/BF00264692
54. May, R. C., & Casadevall, A. (2018). In Fungal Intracellular Pathogenesis, Form Determines Fate. mBio, 9(5), e02092-18. https://doi.org/10.1128/mBio.02092-18
55. Menant, A., Barbey, R., & Thomas, D. (2006). Substrate-mediated remodeling of methionine transport by multiple ubiquitin-dependent mechanisms in yeast cells. The EMBO journal, 25(19), 4436–4447. https://doi.org/10.1038/sj.emboj.7601330
56. Min, K., Neiman, A. M., & Konopka, J. B. (2020). Fungal Pathogens: Shape-Shifting Invaders. Trends in microbiology, 28(11), 922–933. https://doi.org/10.1016/j.tim.2020.05.001
57. Monniot, C., Boisramé, A., Da Costa, G., Chauvel, M., Sautour, M., Bougnoux, M. E., Bellon-Fontaine, M. N., Dalle, F., d'Enfert, C., & Richard, M. L. (2013). Rbt1 protein domains analysis in Candida albicans brings insights into hyphal surface modifications and Rbt1 potential role during adhesion and biofilm formation. PloS one, 8(12), e82395. https://doi.org/10.1371/journal.pone.0082395
58. Moyes, D. L., Wilson, D., Richardson, J. P., Mogavero, S., Tang, S. X., Wernecke, J., Höfs, S., Gratacap, R. L., Robbins, J., Runglall, M., Murciano, C., Blagojevic, M., Thavaraj, S., Förster, T. M., Hebecker, B., Kasper, L., Vizcay, G., Iancu, S. I., Kichik, N., Häder, A., … Naglik, J. R. (2016). Candidalysin is a fungal peptide toxin critical for mucosal infection. Nature, 532(7597), 64–68. https://doi.org/10.1038/nature17625
59. Nantel, A., Dignard, D., Bachewich, C., Harcus, D., Marcil, A., Bouin, A. P., Sensen, C. W., Hogues, H., van het Hoog, M., Gordon, P., Rigby, T., Benoit, F., Tessier, D. C., Thomas, D. Y., & Whiteway, M. (2002). Transcription profiling of Candida albicans cells undergoing the yeast-to-hyphal transition. Molecular biology of the cell, 13(10), 3452–3465. https://doi.org/10.1091/mbc.e02-05-0272
60. Naranjo-Ortiz, M. A., & Gabaldón, T. (2019). Fungal evolution: major ecological adaptations and evolutionary transitions. Biological reviews of the Cambridge Philosophical Society, 94(4), 1443–1476. https://doi.org/10.1111/brv.12510
61. Netea, M. G., Van Der Graaf, C. A., Vonk, A. G., Verschueren, I., Van Der Meer, J. W., & Kullberg, B. J. (2002). The role of toll-like receptor (TLR) 2 and TLR4 in the host defense against disseminated candidiasis. The Journal of infectious diseases, 185(10), 1483–1489. https://doi.org/10.1086/340511
62. Newcomb, L. L., Diderich, J. A., Slattery, M. G., & Heideman, W. (2003). Glucose regulation of Saccharomyces cerevisiae cell cycle genes. Eukaryotic cell, 2(1), 143–149. https://doi.org/10.1128/EC.2.1.143-149.2003
63. Palková, Z., & Váchová, L. (2006). Life within a community: benefit to yeast long-term survival. FEMS microbiology reviews, 30(5), 806–824. https://doi.org/10.1111/j.1574-6976.2006.00034.x
64. Pan, X., Harashima, T., & Heitman, J. (2000). Signal transduction cascades regulating pseudohyphal differentiation of Saccharomyces cerevisiae. Current opinion in microbiology, 3(6), 567–572. https://doi.org/10.1016/s1369-5274(00)00142-9
65. Pappas, P. G., Lionakis, M. S., Arendrup, M. C., Ostrosky-Zeichner, L., & Kullberg, B. J. (2018). Invasive candidiasis. Nature reviews. Disease primers, 4, 18026. https://doi.org/10.1038/nrdp.2018.26
66. Peeters, K., Van Leemputte, F., Fischer, B., Bonini, B. M., Quezada, H., Tsytlonok, M., Haesen, D., Vanthienen, W., Bernardes, N., Gonzalez-Blas, C. B., Janssens, V., Tompa, P., Versées, W., & Thevelein, J. M. (2017). Fructose-1,6-bisphosphate couples glycolytic flux to activation of Ras. Nature communications, 8(1), 922. https://doi.org/10.1038/s41467-017-01019-z
67. Pradhan, B., Guha, D., Ray, P., Das, D., & Aich, P. (2016). Comparative Analysis of the Effects of Two Probiotic Bacterial Strains on Metabolism and Innate Immunity in the RAW 264.7 Murine Macrophage Cell Line. Probiotics and antimicrobial proteins, 8(2), 73–84. https://doi.org/10.1007/s12602-016-9211-4
68. Puumala, E., Fallah, S., Robbins, N., & Cowen, L. E. (2024). Advancements and challenges in antifungal therapeutic development. Clinical microbiology reviews, 37(1), e0014223. https://doi.org/10.1128/cmr.00142-23
69. Reuss, O., Vik, A., Kolter, R., & Morschhäuser, J. (2004). The SAT1 flipper, an optimized tool for gene disruption in Candida albicans. Gene, 341, 119–127. https://doi.org/10.1016/j.gene.2004.06.021

70. Richardson, J. P., Mogavero, S., Moyes, D. L., Blagojevic, M., Krüger, T., Verma, A. H., Coleman, B. M., De La Cruz Diaz, J., Schulz, D., Ponde, N. O., Carrano, G., Kniemeyer, O., Wilson, D., Bader, O., Enoiu, S. I., Ho, J., Kichik, N., Gaffen, S. L., Hube, B., & Naglik, J. R. (2018). Processing of Candida albicans Ece1p Is Critical for Candidalysin Maturation and Fungal Virulence. mBio, 9(1), e02178-17. https://doi.org/10.1128/mBio.02178-17
71. Riquelme, M., Aguirre, J., Bartnicki-García, S., Braus, G. H., Feldbrügge, M., Fleig, U., Hansberg, W., Herrera-Estrella, A., Kämper, J., Kück, U., Mouriño-Pérez, R. R., Takeshita, N., & Fischer, R. (2018). Fungal Morphogenesis, from the Polarized Growth of Hyphae to Complex Reproduction and Infection Structures. Microbiology and molecular biology reviews : MMBR, 82(2), e00068-17. https://doi.org/10.1128/MMBR.00068-17
72. Rolland, F., De Winde, J. H., Lemaire, K., Boles, E., Thevelein, J. M., & Winderickx, J. (2000). Glucose-induced cAMP signalling in yeast requires both a G-protein coupled receptor system for extracellular glucose detection and a separable hexose kinase-dependent sensing process. Molecular microbiology, 38(2), 348–358. https://doi.org/10.1046/j.1365-2958.2000.02125.x
73. Rouillon, A., Barbey, R., Patton, E. E., Tyers, M., & Thomas, D. (2000). Feedback-regulated degradation of the transcriptional activator Met4 is triggered by the SCF(Met30)complex. The EMBO journal, 19(2), 282–294. https://doi.org/10.1093/emboj/19.2.282
74. Ryan, O., Shapiro, R. S., Kurat, C. F., Mayhew, D., Baryshnikova, A., Chin, B., Lin, Z. Y., Cox, M. J., Vizeacoumar, F., Cheung, D., Bahr, S., Tsui, K., Tebbji, F., Sellam, A., Istel, F., Schwarzmüller, T., Reynolds, T. B., Kuchler, K., Gifford, D. K., Whiteway, M., … Boone, C. (2012). Global gene deletion analysis exploring yeast filamentous growth. Science (New York, N.Y.), 337(6100), 1353–1356. https://doi.org/10.1126/science.1224339
75. Sánchez-Martínez, C., & Pérez-Martín, J. (2002). Gpa2, a G-protein alpha subunit required for hyphal development in Candida albicans. Eukaryotic cell, 1(6), 865–874. https://doi.org/10.1128/EC.1.6.865-874.2002
76. Schiestl, R. H., & Gietz, R. D. (1989). High efficiency transformation of intact yeast cells using single stranded nucleic acids as a carrier. Current genetics, 16(5-6), 339–346. https://doi.org/10.1007/BF00340712
77. Schröder, M., Chang, J. S., & Kaufman, R. J. (2000). The unfolded protein response represses nitrogen-starvation induced developmental differentiation in yeast. Genes & development, 14(23), 2962–2975. https://doi.org/10.1101/gad.852300
78. Segal, E., & Frenkel, M. (2018). Experimental in Vivo Models of Candidiasis. Journal of fungi (Basel, Switzerland), 4(1), 21. https://doi.org/10.3390/jof4010021
79. Sexton, A. C., & Howlett, B. J. (2006). Parallels in fungal pathogenesis on plant and animal hosts. Eukaryotic cell, 5(12), 1941–1949. https://doi.org/10.1128/EC.00277-06
80. Sharkey, L. L., McNemar, M. D., Saporito-Irwin, S. M., Sypherd, P. S., & Fonzi, W. A. (1999). HWP1 functions in the morphological development of Candida albicans downstream of EFG1, TUP1, and RBF1. Journal of bacteriology, 181(17), 5273–5279. https://doi.org/10.1128/JB.181.17.5273-5279.1999
81. Shee, S., Singh, S., Tripathi, A., Thakur, C., Kumar T, A., Das, M., Yadav, V., Kohli, S., Rajmani, R. S., Chandra, N., Chakrapani, H., Drlica, K., & Singh, A. (2022). Moxifloxacin-Mediated Killing of Mycobacterium tuberculosis Involves Respiratory Downshift, Reductive Stress, and Accumulation of Reactive Oxygen Species. Antimicrobial agents and chemotherapy, 66(9), e0059222. https://doi.org/10.1128/aac.00592-22
82. Shrivastava, M., Feng, J., Coles, M., Clark, B., Islam, A., Dumeaux, V., & Whiteway, M. (2021). Modulation of the complex regulatory network for methionine biosynthesis in fungi. Genetics, 217(2), iyaa049. https://doi.org/10.1093/genetics/iyaa049
83. Smith, M. G., Des Etages, S. G., & Snyder, M. (2004). Microbial synergy via an ethanol-triggered pathway. Molecular and cellular biology, 24(9), 3874–3884. https://doi.org/10.1128/MCB.24.9.3874-3884.2004
84. Smothers, D. B., Kozubowski, L., Dixon, C., Goebl, M. G., & Mathias, N. (2000). The abundance of Met30p limits SCF(Met30p) complex activity and is regulated by methionine availability. Molecular and cellular biology, 20(21), 7845–7852. https://doi.org/10.1128/MCB.20.21.7845-7852.2000
85. Song, Y., Li, S., Zhao, Y., Zhang, Y., Lv, Y., Jiang, Y., Wang, Y., Li, D., & Zhang, H. (2019). ADH1 promotes Candida albicans pathogenicity by stimulating oxidative phosphorylation. International journal of medical microbiology : IJMM, 309(6), 151330. https://doi.org/10.1016/j.ijmm.2019.151330

86. Strudwick, N., Brown, M., Parmar, V. M., & Schröder, M. (2010). Ime1 and Ime2 are required for pseudohyphal growth of Saccharomyces cerevisiae on nonfermentable carbon sources. Molecular and cellular biology, 30(23), 5514–5530. https://doi.org/10.1128/MCB.00390-10
87. Su, C., Yu, J., Sun, Q., Liu, Q., & Lu, Y. (2018). Hyphal induction under the condition without inoculation in Candida albicans is triggered by Brg1-mediated removal of NRG1 inhibition. Molecular microbiology, 108(4), 410–423. https://doi.org/10.1111/mmi.13944
88. Su, N. Y., Ouni, I., Papagiannis, C. V., & Kaiser, P. (2008). A dominant suppressor mutation of the met30 cell cycle defect suggests regulation of the Saccharomyces cerevisiae Met4-Cbf1 transcription complex by Met32. The Journal of biological chemistry, 283(17), 11615–11624. https://doi.org/10.1074/jbc.M708230200
89. Thomas, D., & Surdin-Kerjan, Y. (1997). Metabolism of sulfur amino acids in Saccharomyces cerevisiae. Microbiology and molecular biology reviews : MMBR, 61(4), 503–532. https://doi.org/10.1128/mmbr.61.4.503-532.1997
90. Thompson, D. S., Carlisle, P. L., & Kadosh, D. (2011). Coevolution of morphology and virulence in Candida species. Eukaryotic cell, 10(9), 1173–1182. https://doi.org/10.1128/EC.05085-11
91. Uwamahoro, N., Verma-Gaur, J., Shen, H. H., Qu, Y., Lewis, R., Lu, J., Bambery, K., Masters, S. L., Vince, J. E., Naderer, T., & Traven, A. (2014). The pathogen Candida albicans hijacks pyroptosis for escape from macrophages. mBio, 5(2), e00003–e14. https://doi.org/10.1128/mBio.00003-14
92. Van de Velde, S., & Thevelein, J. M. (2008). Cyclic AMP-protein kinase A and Snf1 signaling mechanisms underlie the superior potency of sucrose for induction of filamentation in Saccharomyces cerevisiae. Eukaryotic cell, 7(2), 286–293. https://doi.org/10.1128/EC.00276-07
93. Wang, L., & Lin, X. (2012). Morphogenesis in fungal pathogenicity: shape, size, and surface. PLoS pathogens, 8(12), e1003027. https://doi.org/10.1371/journal.ppat.1003027
94. Wilson, D., Naglik, J. R., & Hube, B. (2016). The Missing Link between Candida albicans Hyphal Morphogenesis and Host Cell Damage. PLoS pathogens, 12(10), e1005867. https://doi.org/10.1371/journal.ppat.1005867
95. Winer, J., Jung, C. K., Shackel, I., & Williams, P. M. (1999). Development and validation of real-time quantitative reverse transcriptase-polymerase chain reaction for monitoring gene expression in cardiac myocytes in vitro. Analytical biochemistry, 270(1), 41–49. https://doi.org/10.1006/abio.1999.4085
96. Wu, J., Zhang, N., Hayes, A., Panoutsopoulou, K., & Oliver, S. G. (2004). Global analysis of nutrient control of gene expression in Saccharomyces cerevisiae during growth and starvation. Proceedings of the National Academy of Sciences of the United States of America, 101(9), 3148–3153. https://doi.org/10.1073/pnas.0308321100
97. Wu, Y., Zhang, S., Gong, X., Yu, Q., Zhang, Y., Luo, M., Zhang, X., Workman, J. L., Yu, X., & Li, S. (2019). Glycolysis regulates gene expression by promoting the crosstalk between H3K4 trimethylation and H3K14 acetylation in Saccharomyces cerevisiae. Journal of genetics and genomics = Yi chuan xue bao, 46(12), 561–574. https://doi.org/10.1016/j.jgg.2019.11.007
98. Xue, Y., Batlle, M., & Hirsch, J. P. (1998). GPR1 encodes a putative G protein-coupled receptor that associates with the Gpa2p Galpha subunit and functions in a Ras-independent pathway. The EMBO journal, 17(7), 1996–2007. https://doi.org/10.1093/emboj/17.7.1996
99. Yen, J. L., Su, N. Y., & Kaiser, P. (2005). The yeast ubiquitin ligase SCFMet30 regulates heavy metal response. Molecular biology of the cell, 16(4), 1872–1882. https://doi.org/10.1091/mbc.e04-12-1130
100. Yoshino, M., & Murakami, K. (1982). AMP deaminase as a control system of glycolysis in yeast. Mechanism of the inhibition of glycolysis by fatty acid and citrate. The Journal of biological chemistry, 257(18), 10644–10649. https://doi.org/10.1016/S0021-9258(19)81037-2
101. Yun, C. W., Tamaki, H., Nakayama, R., Yamamoto, K., & Kumagai, H. (1997). G-protein coupled receptor from yeast Saccharomyces cerevisiae. Biochemical and biophysical research communications, 240(2), 287–292. https://doi.org/10.1006/bbrc.1997.7649

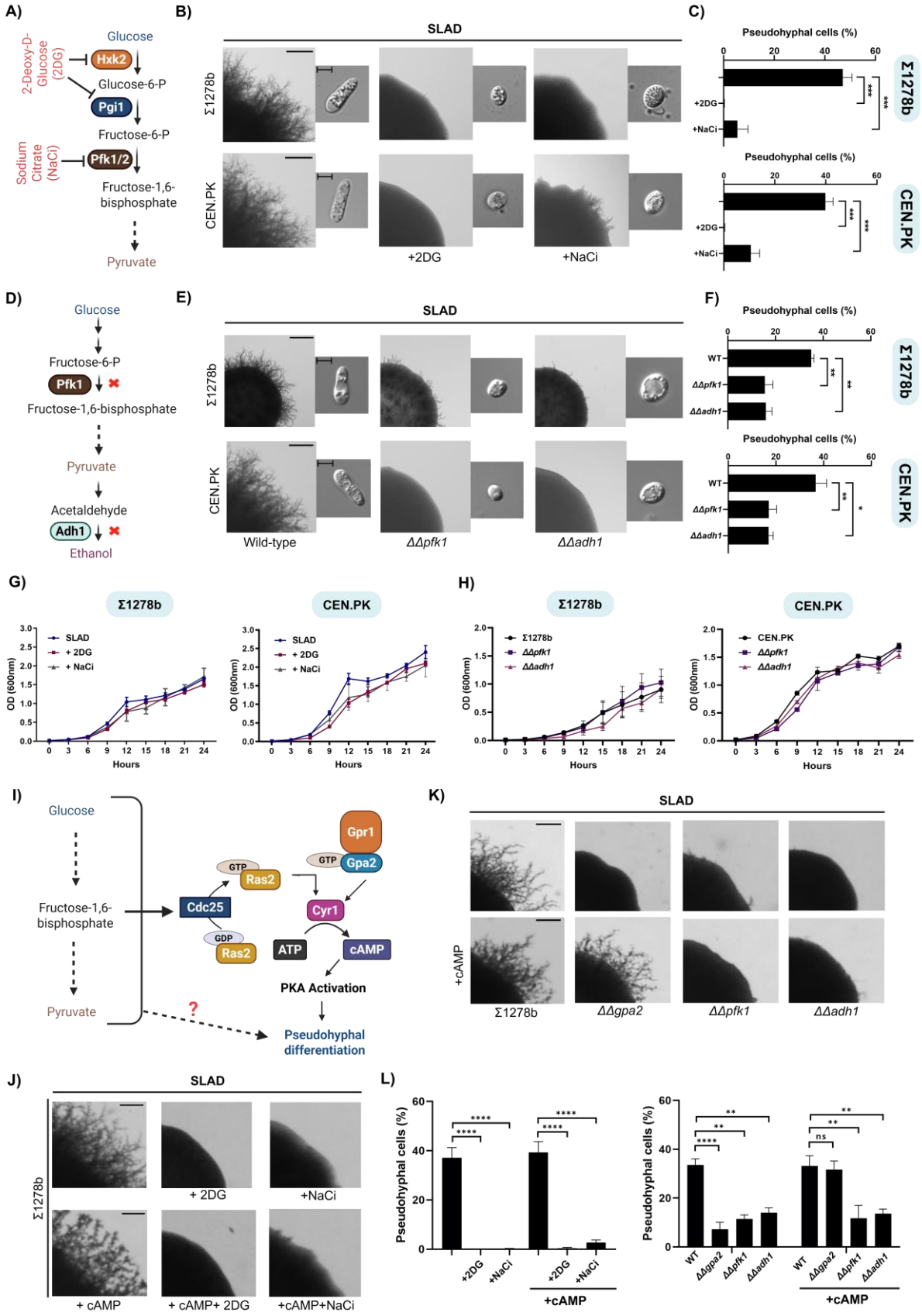
A)
Glucose
2-Deoxy-D-Glucose (2DG)
Hxk2
Glucose-6-P
Pgi1
Fructose-6-P
Sodium Citrate (NaCi)
Pfk1/2
Fructose-1,6-bisphosphate
Pyruvate
B)
SLAD
Σ1278b
CEN.PK
+2DG
+NaCi
C)
Pseudohyphal cells (%)
Σ1278b
CEN.PK
D)
Glucose
Fructose-6-P
Pfk1
Fructose-1,6-bisphosphate
Pyruvate
Acetaldehyde
Adh1
Ethanol
E)
SLAD
Wild-type
ΔΔpfk1
ΔΔadh1
F)
WT
G)
Σ1278b
CEN.PK
SLAD
+ 2DG
+ NaCi
OD (600nm)
Hours
H)
ΔΔpfk1
ΔΔadh1
I)
Glucose
Fructose-1,6-bisphosphate
Pyruvate
Gpr1
Gpa2
GTP
Ras2
Cdc25
GDP
Cyr1
ATP
cAMP
PKA Activation
Pseudohyphal differentiation
K)
SLAD
+cAMP
Σ1278b
ΔΔgpa2
ΔΔpfk1
ΔΔadh1
J)
SLAD
Σ1278b
+ 2DG
+NaCi
+ cAMP
+ cAMP+ 2DG
+cAMP+NaCi
L)
Pseudohyphal cells (%)
+2DG
+NaCi
+cAMP
WT
ΔΔgpa2
ΔΔpfk1
ΔΔadh1

Figure 1. Glycolysis is Critical for Pseudohyphal Differentiation in a cAMP-PKA Independent Manner in *S. cerevisiae*.

(A) Schematic overview of glycolysis and its inhibition by glycolysis inhibitors (2-Deoxy-D-Glucose (2DG) and sodium citrate (NaCi)). **(B)** Wild-type ∑1278b or CEN.PK were spotted on nitrogen-limiting medium containing 2% (w/v) glucose (SLAD) with and without sub-inhibitory concentrations of glycolysis inhibitors (2DG or NaCi), incubated for 10 days at 30 °C. Scale bar represents 1mm for whole colony images and 5µm for single cell images. **(C)** Cells from colonies were isolated and length/width ratio of individual cells was measured using ImageJ and percentage of pseudohyphal cells from total population was determined. More than 500 cells were counted for each condition. Statistical analysis was done using one-way ANOVA test, ***(P<0.001). Error bars represent SEM. **(D)** Schematic overview of glycolysis showing targeted gene deletions. **(E)** Pertinent knockout strains which lack genes encoding for enzymes involved in glycolysis such as *pfk1* and *adh1* were spotted on SLAD along with wild-type ∑1278b or CEN.PK. Scale bar represents 1mm for whole colony images and 5µm for single cell images. **(F)** Cells from colonies were isolated and single cells were imaged using Zeiss Apotome microscope length/width ratio of individual cells was measured using ImageJ and percentage of pseudohyphal cells from total population was determined. More than 500 cells were counted for each strains. Statistical analysis was done using one-way ANOVA test, **(P<0.01) and *(P<0.05). Error bars represent SEM. **(G)** Growth curve was performed to monitor overall growth of wild-type strains on SLAD, SLAD+2DG and SLAD+NaCi. Overnight grown culture of wild-type strains (∑1278b or CEN.PK) were diluted to OD_{600}=0.01 in fresh SLAD medium with and without 2DG (0.05% w/v) or NaCi (0.5% w/v) and allowed to grow at 30 °C for 24 hours. OD_{600} was recorded at 3-h intervals **(H)** Growth curve was performed to monitor overall growth of wild-type and knockout strains on SLAD. Overnight grown culture of deletion strains (*ΔΔpfk1* or *ΔΔadh1*) along with wild-type strains (∑1278b or CEN.PK) were diluted to OD_{600}=0.01 in fresh SLAD and allowed to grow at 30 °C for 24 hours. OD_{600} was recorded at 3-h intervals. **(I)** Schematic overview of the role of glucose and glycolytic intermediates in the activation of cAMP-PKA pathway during pseudohyphal differentiation. **(J)** Wild-type ∑1278b was spotted on SLAD containing sub-inhibitory concentration of 2DG or NaCi with and without cAMP (1mM), incubated for 10 days at 30 °C. Scale bar represents 1mm for whole colony images. **(K)** Pertinent knockout strains which lack genes that encode for enzymes involved in glycolysis such as *pfk1* and *adh1* were spotted on SLAD with and without cAMP (1mM), incubated for 10 days at 30 °C. *ΔΔgpa2* strain was used as a control. Scale bar represents 1mm for whole colony images. **(L)** Cells from colonies were isolated and length/width ratio of individual cells was measured using ImageJ and percentage of pseudohyphal cells from total population was determined. More than 500 cells were counted for each condition. Statistical analysis was done using one-way ANOVA test, ****(P<0.0001), **(P<0.01) and ns(non-significant). Error bars represent SEM. This figure was created using Biorender.com

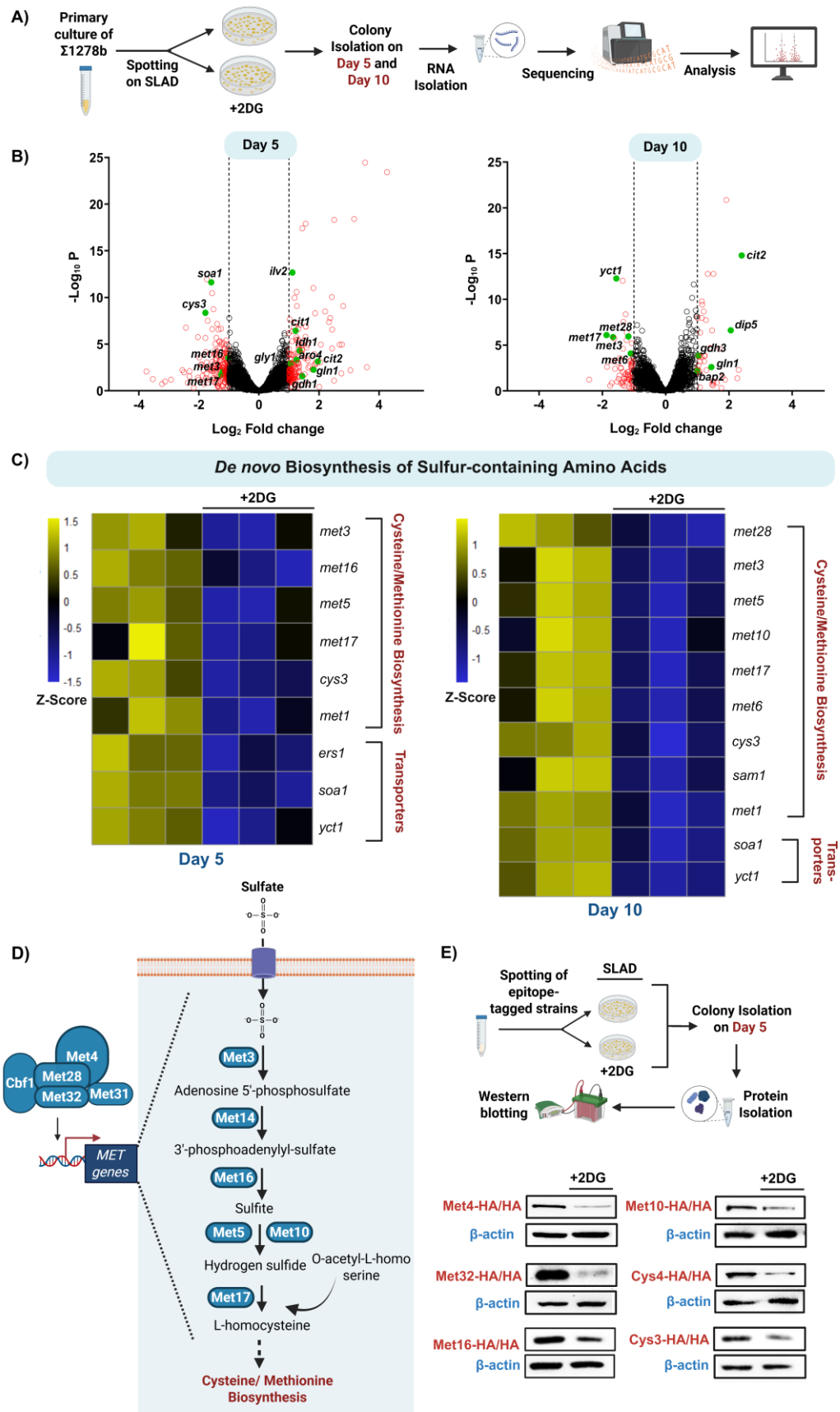
A)
Primary culture of Σ1278b
Spotting on SLAD
+2DG
Colony Isolation on Day 5 and Day 10
RNA Isolation
Sequencing
Analysis
B)
Day 5
Day 10
-Log10 P
Log2 Fold change
soa1
cys3
ilv2
cit1
idh1
aro4
cit2
gln1
gdh1
met16
met3
met17
gly1
yct1
cit2
dip5
met28
met17
met3
met6
gdh3
gln1
bap2
C)
De novo Biosynthesis of Sulfur-containing Amino Acids
+2DG
Z-Score
met3
met16
met5
met17
cys3
met1
ers1
soa1
yct1
Cysteine/Methionine Biosynthesis
Transporters
Day 5
met28
met3
met5
met10
met17
met6
cys3
sam1
met1
soa1
yct1
Trans-porters
Day 10
D)
Sulfate
Met4
Cbf1
Met28
Met32
Met31
MET genes
Met3
Adenosine 5'-phosphosulfate
Met14
3'-phosphoadenylyl-sulfate
Met16
Sulfite
Met5
Met10
Hydrogen sulfide
O-acetyl-L-homo serine
Met17
L-homocysteine
Cysteine/ Methionine Biosynthesis
E)
Spotting of epitope-tagged strains
SLAD
+2DG
Colony Isolation on Day 5
Protein Isolation
Western blotting
+2DG
Met4-HA/HA
β-actin
Met32-HA/HA
β-actin
Met16-HA/HA
β-actin
+2DG
Met10-HA/HA
β-actin
Cys4-HA/HA
β-actin
Cys3-HA/HA
β-actin

Figure 2. Comparative Transcriptomics Identifies the Role of Glycolysis in Regulating Sulfur Metabolism During Pseudohyphal Differentiation in *S. cerevisiae*.

(A) Schematic overview of steps involved in RNA isolation and sequencing. **(B)** Volcano plots represent differentially expressed genes in 2DG treated cells compared to untreated cells isolated from D-5 and D-10 colonies, respectively. Genes which are upregulated (Log_2 fold change ≥ 1) and downregulated (Log_2 fold change ≤ -1) are highlighted in red. Some of the significantly upregulated and downregulated genes involved in the biosynthesis of various amino acids are highlighted in green. **(C)** Heatmaps represent the differentially expressed genes involved in *de novo* biosynthesis and transport of sulfur-containing amino acids, in 2DG treated cells compared to untreated cells isolated from D-5 and D-10 colonies, respectively (n=3). Scale bar represents Z-Score. **(D)** Schematic overview of *de novo* biosynthesis of sulfur-containing amino acids. **(E)** Schematic overview of steps involved in the Western blotting experiments. Epitope-tagged strains of various proteins involved in the *de novo* biosynthesis of sulfur-containing amino acids including Met4, Met32, Met16, Met10, Cys4 and Cys3 were spotted on SLAD in the presence and absence of sub-inhibitory concentration of 2DG following which, cells from colonies were isolated on D-5 and levels of these proteins were assessed using Western blotting. β-actin was used as loading control. This figure was created using Biorender.com

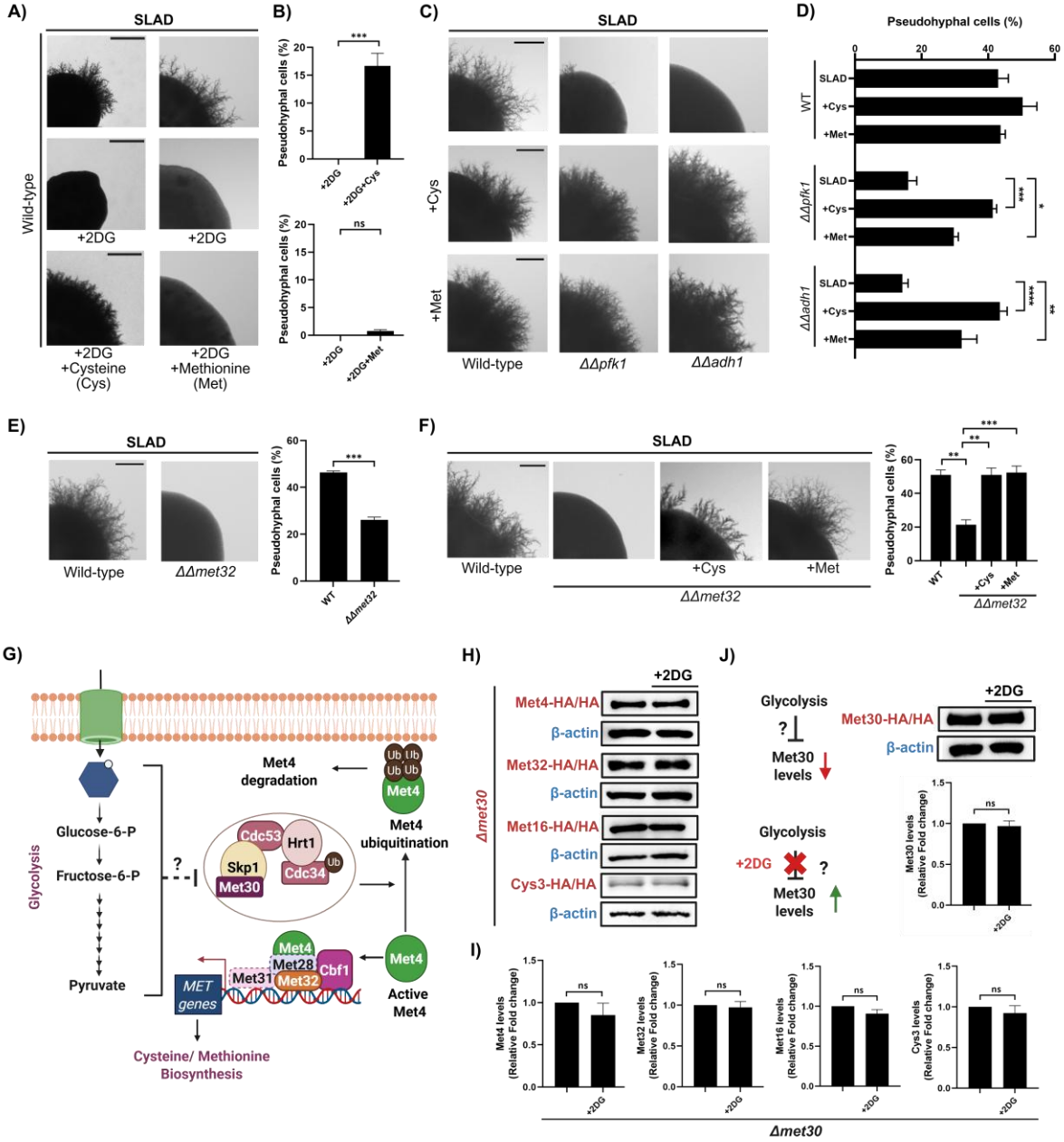

Figure 3. Glycolysis-mediated Regulation of Sulfur Metabolism is Critical for Pseudohyphal Differentiation in *S. cerevisiae*.

(A) Wild-type ∑1278b was spotted on SLAD containing sub-inhibitory concentration of 2DG with and without sulfur-containing compounds including cysteine (500μM) or methionine (20μM), incubated for 10 days at 30 °C. Scale bar represents 1mm for whole colony images. **(B)** Cells from colonies were isolated and length/width ratio of individual cells was measured using ImageJ and percentage of pseudohyphal cells from total population was determined. More than 500 cells were counted for each condition. Statistical analysis was done using unpaired t-test, ***(P<0.001) and ns (non-significant). Error bars represent SEM. **(C)** Pertinent knockout strains (*ΔΔpfk1* or *ΔΔadh1*) along with wild-type were spotted on SLAD with and without sulfur-containing compounds including cysteine (200μM) or methionine (20μM), incubated for 10 days at 30 °C. Scale bar represents 1mm for whole colony images. **(D)** Cells from colonies were isolated and length/width ratio of individual cells was measured using ImageJ and percentage of pseudohyphal cells from total population was determined. More than 500 cells were counted for each condition. Statistical analysis was done using

one-way ANOVA test, ****(P<0.0001), ***(P<0.001), **(P<0.01) and *(P<0.05). Error bars represent SEM. **(E)** Pertinent knockout strains which lack genes encoding for transcription factor involved in *de novo* biosynthesis of sulfur-containing amino acids including *met32* along with wild-type ∑1278b were spotted on SLAD. Scale bar represents 1mm for whole colony images. Cells from colonies were isolated and length/width ratio of individual cells was measured using ImageJ and percentage of pseudohyphal cells from total population was determined. More than 500 cells were counted for each condition. Statistical analysis was done using unpaired t-test, ***(P<0.001). Error bars represent SEM. **(F)** Pertinent knockout strain (*ΔΔmet32)* was spotted on SLAD with and without sulfur-containing compounds including cysteine (200μM) or methionine (20μM), incubated for 10 days at 30 °C. Wild-type spotted on SLAD was used as control. Scale bar represents 1mm for whole colony images. Cells from colonies were isolated and length/width ratio of individual cells was measured using ImageJ and percentage of pseudohyphal cells from total population was determined. More than 500 cells were counted for each condition. Statistical analysis was done using one-way ANOVA test, ***(P<0.001) and **(P<0.01). Error bars represent SEM. **(G)** Schematic overview of the proposed role of SCF^{Met30} in glycolysis-dependent regulation of sulfur metabolism during pseudohyphal differentiation under nitrogen-limiting conditions in *S. cerevisiae.* **(H)** Epitope-tagged strains of various proteins involved in the *de novo* biosynthesis of sulfur-containing amino acids including Met4, Met32, Met16 and Cys3 in *Δmet30* background were spotted on SLAD in the presence and absence of sub-inhibitory concentration of 2DG following which, cells from colonies were isolated on D-5 and levels of these proteins were assessed using Western blotting. β-actin was used as loading control. **(I)** Raw images of Western blots were analysed using ImageJ to normalize targeted protein expression with the expression of housekeeping protein- β-actin, in order to generate densitometric graphs. Statistical analysis was done using unpaired t-test, ns (non-significant). Error bars represent SEM. **(J)** Epitope-tagged strain of Met30 was spotted on SLAD in the presence and absence of sub-inhibitory concentration of 2DG following which, cells from colonies were isolated on D-5 and levels of these proteins were assessed using Western blotting. β-actin was used as loading control. Raw images of Western blots were analysed using ImageJ to normalize targeted protein expression with the expression of housekeeping protein- β-actin, in order to generate densitometric graphs. Statistical analysis was done using unpaired t-test, ns (non-significant). Error bars represent SEM. This figure was created using Biorender.com

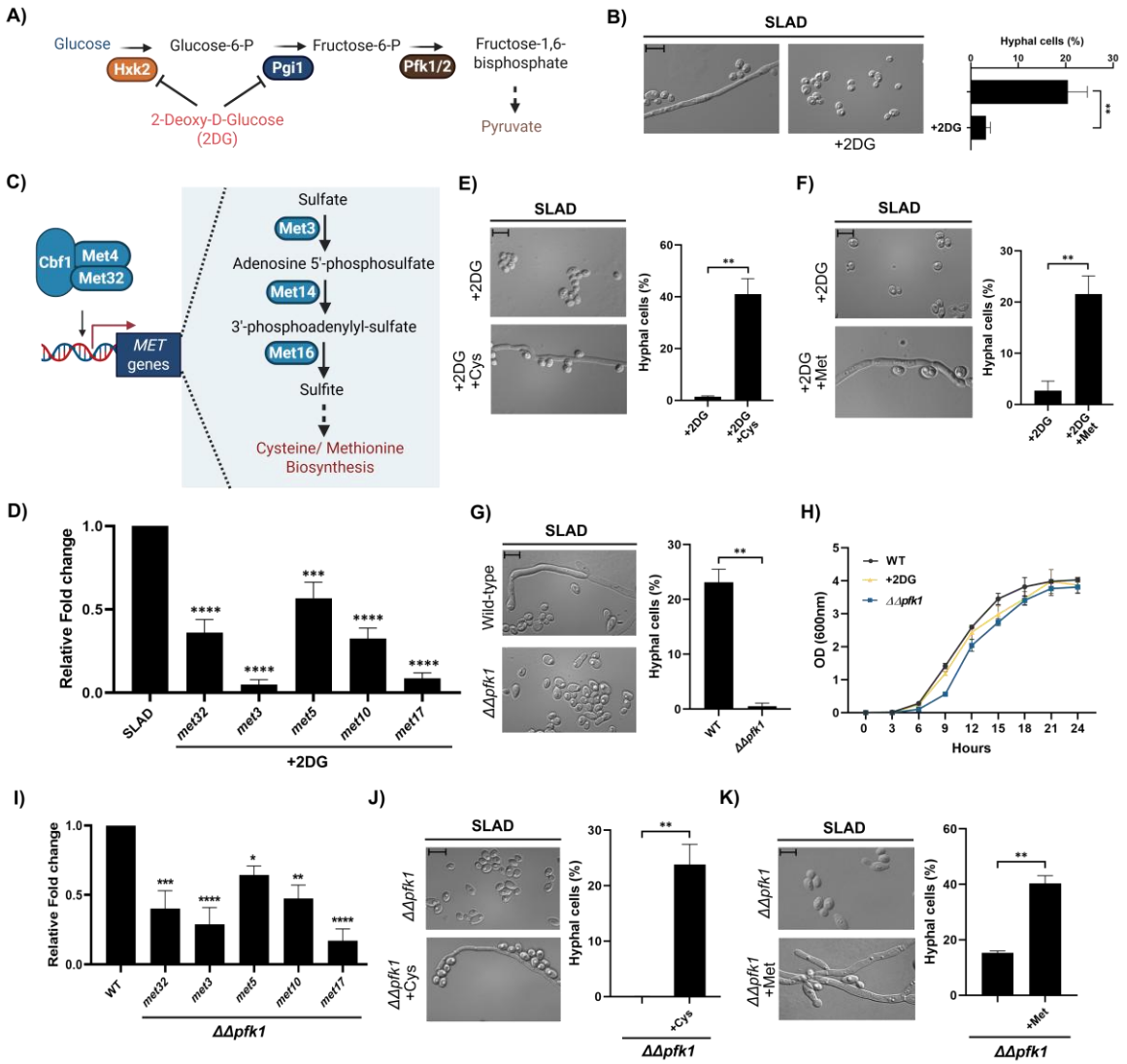

Figure 4. Glycolysis-dependent Sulfur Metabolism is Critical for Hyphal Differentiation in *C. albicans*.

(A) Schematic overview of glycolysis and its inhibition by glycolysis inhibitor (2DG). **(B)** Wild-type SC5314 was spotted on SLAD with and without sub-inhibitory concentration of glycolysis inhibitor 2DG, incubated for 7 days at 37 °C. Cells from colonies were isolated and length/width ratio of individual cells was measured using ImageJ and percentage of hyphal cells from total population was determined. More than 500 cells were counted for each condition. Scale bar represents 10μm for single cell images. Statistical analysis was done using unpaired t-test, **(P<0.01). Error bars represent SEM. **(C)** Schematic overview of *de novo* biosynthesis of sulfur-containing amino acids. **(D)** Wild-type SC5314 was spotted on SLAD, in the presence and absence of sub-inhibitory concentration of 2DG and cells from colonies were isolated after ~4 days, for RNA isolation. We then performed comparative RT-qPCR to check for the relative expression of genes involved in the *de novo* biosynthesis of sulfur-containing amino acids pathway including *met32*, *met3*, *met5* (*ecm17*), *met10* and *met17* (*met15*). Statistical analysis was done using one-way ANOVA test, ****(P<0.0001) and ***(P<0.001). Error bars represent SEM. **(E)** Wild-type SC5314 was spotted on SLAD containing sub-inhibitory concentration of 2DG with and without cysteine (100μM) and, incubated for 7 days at 37 °C. Cells from colonies were isolated and length/width ratio of individual cells was measured using ImageJ and percentage of hyphal cells from total population was determined. Scale bar represents 10μm for single cell images. More than 500 cells were counted for

each condition. Statistical analysis was done using unpaired t-test, **(P<0.01). Error bars represent SEM. **(F)** Wild-type SC5314 was spotted on SLAD containing sub-inhibitory concentration of 2DG with and without methionine (20μM) and, incubated for 7 days at 37 °C. Cells from colonies were isolated and length/width ratio of individual cells was measured using ImageJ and percentage of hyphal cells from total population was determined. More than 500 cells were counted for each condition. Scale bar represents 10μm for single cell images. Statistical analysis was done using unpaired t-test, **(P<0.01). Error bars represent SEM. **(G)** Wild-type SC5314 and pertinent knockout strain which lacks the genes encoding for a glycolytic enzyme, *pfk1* (*ΔΔpfk1*) were spotted on SLAD, incubated for 7 days at 37 °C. Cells from colonies were isolated and length/width ratio of individual cells was measured using ImageJ and percentage of hyphal cells from total population was determined. Scale bar represents 10μm for single cell images. More than 500 cells were counted for each strain. Statistical analysis was done using unpaired t-test, **(P<0.01). Error bars represent SEM. **(H)** Growth curve was performed to monitor overall growth of wild-type strain on SLAD and SLAD+2DG and *ΔΔpfk1* on SLAD. Overnight grown culture of wild-type strain (SC5314) were diluted to OD_{600}=0.01 in fresh SLAD medium with and without 2DG (0.2% (w/v)) and allowed to grow at 30 °C for 24 hours. OD_{600} was recorded at 3-h intervals. For *ΔΔpfk1*, overnight grown culture of *ΔΔpfk1* strains along with wild-type strain (SC5314) were diluted to OD_{600}=0.01 in fresh SLAD and allowed to grow at 30 °C for 24 hours. OD_{600} was recorded at 3-h intervals. **(I)** *ΔΔpfk1* along with Wild-type SC5314 was spotted on SLAD and cells from colonies were isolated after ~4 days, for RNA isolation. We then performed comparative RT-qPCR to check for the relative expression of genes involved in the *de novo* biosynthesis of sulfur-containing amino acids pathway including *met32*, *met3*, *met5* (*ecm17*), *met10* and *met17* (*met15*). Statistical analysis was done using one-way ANOVA test, ****(P<0.0001), ***(P<0.001), **(P<0.01) and *(P<0.05). Error bars represent SEM. **(J)** *ΔΔpfk1* was spotted on SLAD in the presence and absence of cysteine (100μM), incubated for 7 days at 37 °C. Cells from colonies were isolated and length/width ratio of individual cells was measured using ImageJ and percentage of hyphal cells from total population was determined. More than 500 cells were counted for each condition. Statistical analysis was done using unpaired t-test, **(P<0.01). Error bars represent SEM. **(K)** *ΔΔpfk1* was spotted on SLAD in the presence and absence of methionine (10μM), incubated for 7 days at 37 °C. Cells from colonies were isolated and length/width ratio of individual cells was measured using ImageJ and percentage of hyphal cells from total population was determined. More than 500 cells were counted for each condition. Statistical analysis was done using unpaired t-test, **(P<0.01). Error bars represent SEM. This figure was created using Biorender.com

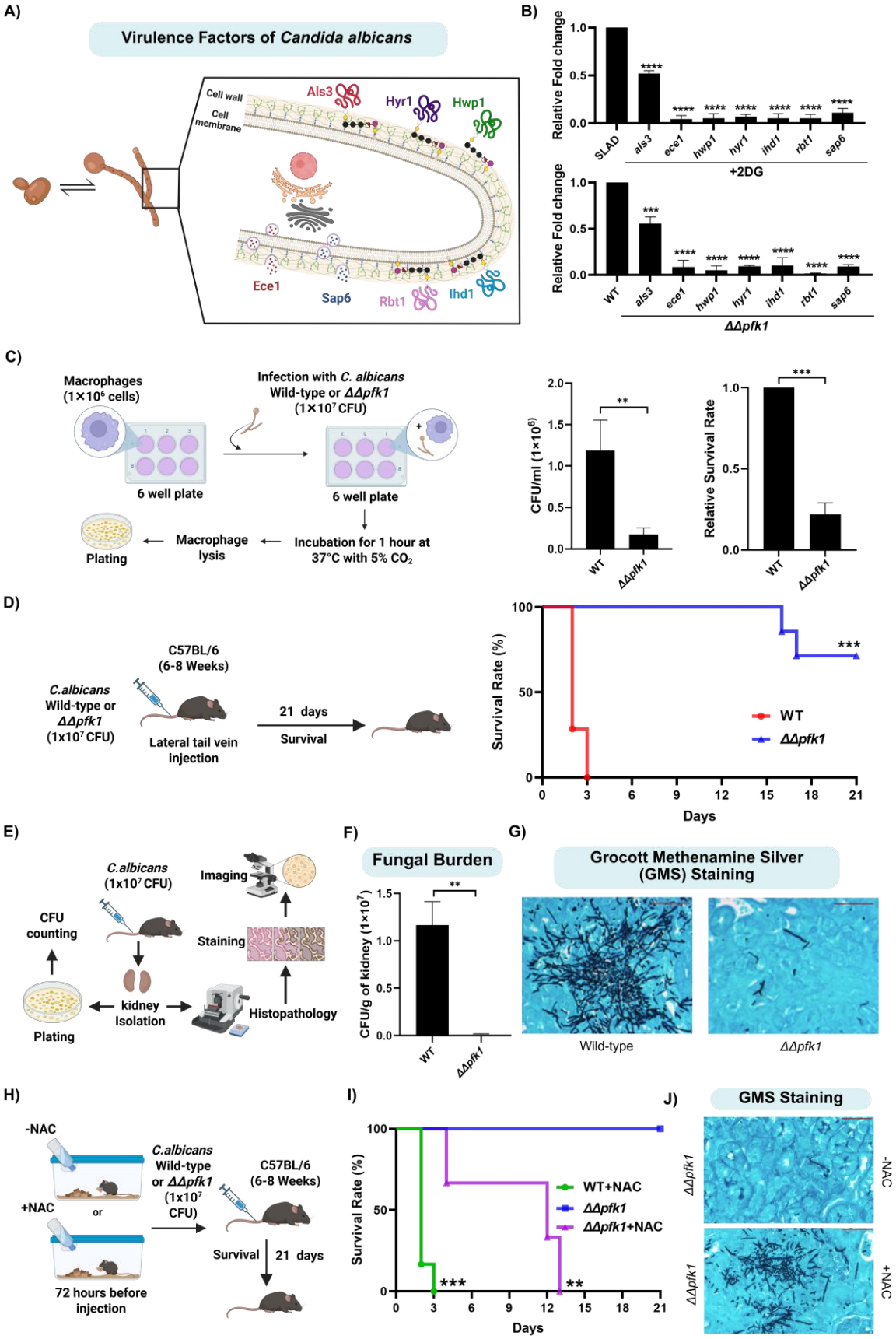

1882
1883
1884

1885 **Figure 5. Perturbation of Glycolysis Leads to Attenuated Fungal Virulence in *C. albicans*.**
1886
1887 **(A)** Schematic overview of various proteins involved in hyphal differentiation and virulence of
1888 *C. albicans*. **(B)** Wild-type SC5314 was spotted on SLAD, in the presence and absence of sub-
1889 inhibitory concentration of 2DG or wild-type SC5314 and *ΔΔpfk1* were spotted on SLAD and cells
1890 from these colonies were isolated after ~4 days, for RNA isolation. We then performed comparative
1891 RT-qPCR to check for the relative expression of genes involved in hyphal differentiation and virulence
1892 of *C. albicans* including *als3, ece1, hwp1, hyr1, ihd1, rbt1* and *sap6.* Statistical analysis was done
1893 using one-way ANOVA test, ****(P<0.0001) and ***(P<0.001). Error bars represent SEM.
1894 **(C)** Schematic overview of *in vitro* microbial survival assay. *RAW 264.7* macrophages were incubated
1895 with the wild-type and *ΔΔpfk1* strain with MOI=10. After 1 hour of incubation, macrophages were
1896 lysed and plating was done to enumerate CFU. Percentage of survival was expressed as the number
1897 of CFU in the presence of macrophages divided by the number of CFU in the absence of macrophages.
1898 Statistical analysis was done using unpaired t-test, ***(P<0.001) and **(P<0.01). Error bars
1899 represent SEM. **(D)** 6-8-week-old C57BL/6 mice were infected intravenously *via* lateral tail vein
1900 injection with 1×10^7 CFU of wild-type SC5314 or 1×10^7 CFU of *ΔΔpfk1*. To determine survival rate,
1901 mice were monitored for 21 days post-infection for clinical signs of illness or mortality. The results
1902 are representative of seven mice per injected strain. Survival percentage were statistically evaluated
1903 by the Log-rank Mantel-Cox test, ***(P<0.001) (n=7). **(E)** Schematic overview of kidney isolation
1904 to check fungal burden using CFU counting and histology. **(F)** Fungal burden was measured by CFU
1905 counting after kidney isolation from mice injected with either wild-type or *ΔΔpfk1*. Statistical analysis
1906 was done using unpaired t-test, **(P<0.01). Error bars represent SEM. **(G)** Histopathological
1907 analysis of kidney sections using Grocott Methanamine Silver (GMS) staining was done for kidneys
1908 isolated from mice injected with either wild-type SC5314 or *ΔΔpfk1*. Fungal cells appear black in
1909 colour against the colored background of the kidney tissue. Bright field imaging was done using
1910 Axioplan 2 microscope at 40X magnification. Scale bar represents 50µm. **(H)** Schematic overview
1911 of N-acetyl cysteine (NAC) administration to mice. **(I)** 6mg/ml of NAC was dissolved in distilled
1912 water and administered orally to 6-8-week-old C57BL/6 mice before 72 hours of *C. albicans* infection.
1913 Mice administered with normal distilled water were used as controls. After 72 hours of treatment,
1914 mice were infected intravenously *via* lateral tail vein injection with 1×10^7 CFU of SC5314 or
1915 1×10^7 CFU of *ΔΔpfk1*. To determine survival rate, mice were monitored for 21 days post-infection
1916 for clinical signs of illness or mortality. The results are representative of six mice per condition.
1917 Survival percentage were statistically evaluated by the Log-rank Mantel-Cox test, ***(P<0.001) and
1918 **(P<0.01) (n=6). **(J)** Histopathological analysis of kidney sections using GMS staining was done
1919 for kidneys isolated from mice administrated with normal distilled water or NAC containing distilled
1920 water and injected with *ΔΔpfk1*. Fungal cells appear black in colour against the colored background
1921 of the kidney tissue. Bright field imaging was done using Axioplan 2 microscope at 40X magnification.
1922 Scale bar represents 50µm. This figure was created using Biorender.com
1923
1924
1925
1926
1927
1928
1929
1930
1931
1932
1933
1934

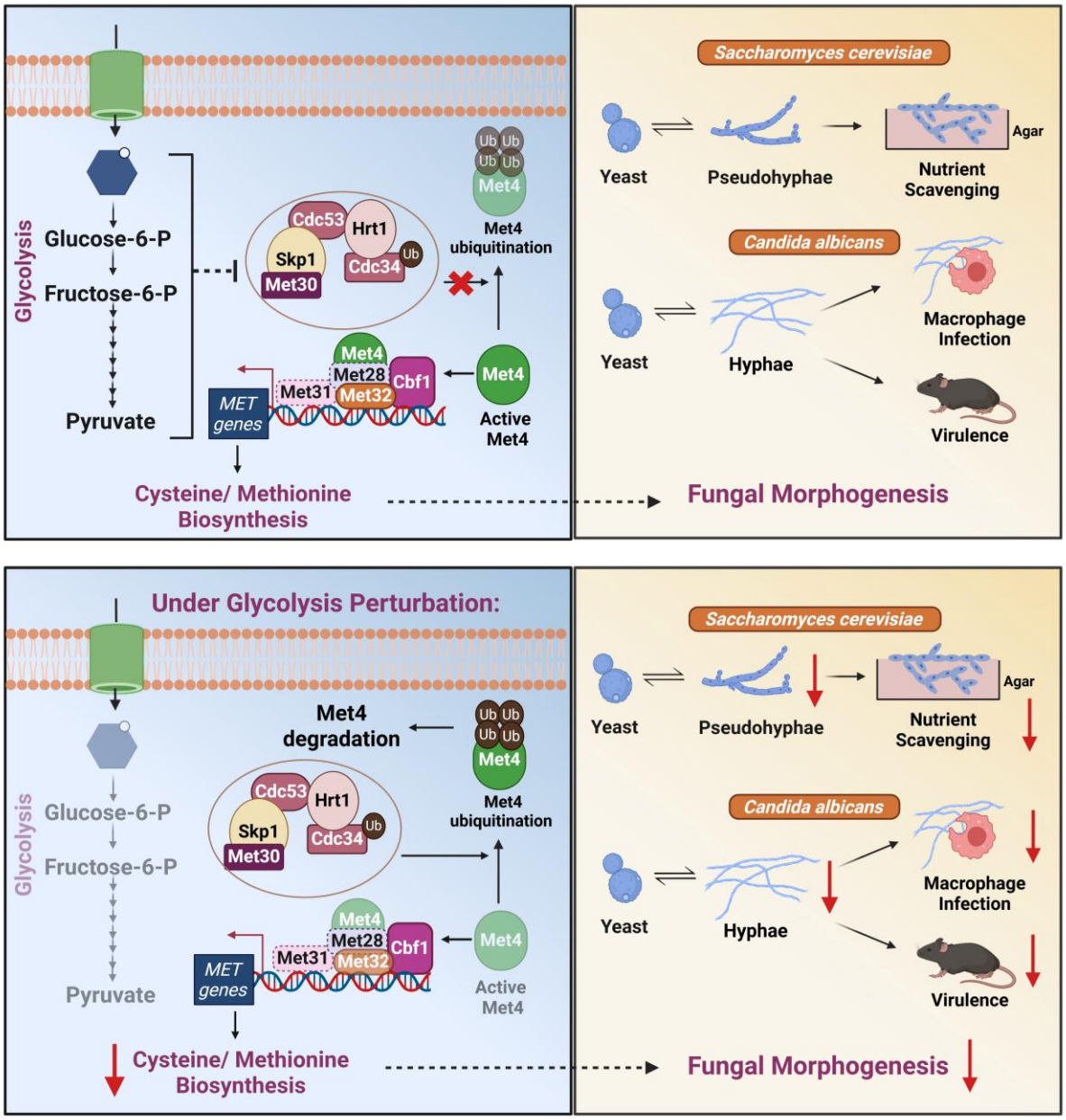

Figure 6. Glycolysis-dependent Sulfur Metabolism Orchestrates Morphological Transitions and Virulence in Fungi.

Active glycolysis plays a key regulatory role in the *de novo* biosynthesis of sulfur-containing amino acids by modulating the activity of SCF^{Met30} complex (SCF^{Met30} complex includes Met30, Skp1, Cdc53, Hrt1 and Cdc34) which in turn affects the expression of genes involved in this process (In *S. cerevisiae*, *MET* transcription complex includes Met4, Met28, Cbf1, Met31, and Met32, whereas in *C. albicans*, the characterized components of this complex include Met4, Cbf1, and Met32. Hence, Met28 and Met31, unique to the *MET* transcription complex of *S. cerevisiae* are represented with dotted borders). Glycolysis-dependent sulfur metabolism in turn, is critical for fungal morphogenesis in both species and the ability of *C. albicans* to survive within macrophages and cause systemic infection in a *murine* model of candidiasis. Perturbation of active glycolysis increases Met30 activity, which leads to the increased degradation of Met4, resulting in the reduced expression of genes involved in the *de novo* biosynthesis of sulfur-containing amino acids. This in turn attenuates fungal morphogenesis in both species and the ability of *C. albicans* to survive within macrophages and cause systemic infection in a *murine* model of candidiasis. This figure was created using Biorender.com

Supporting Information

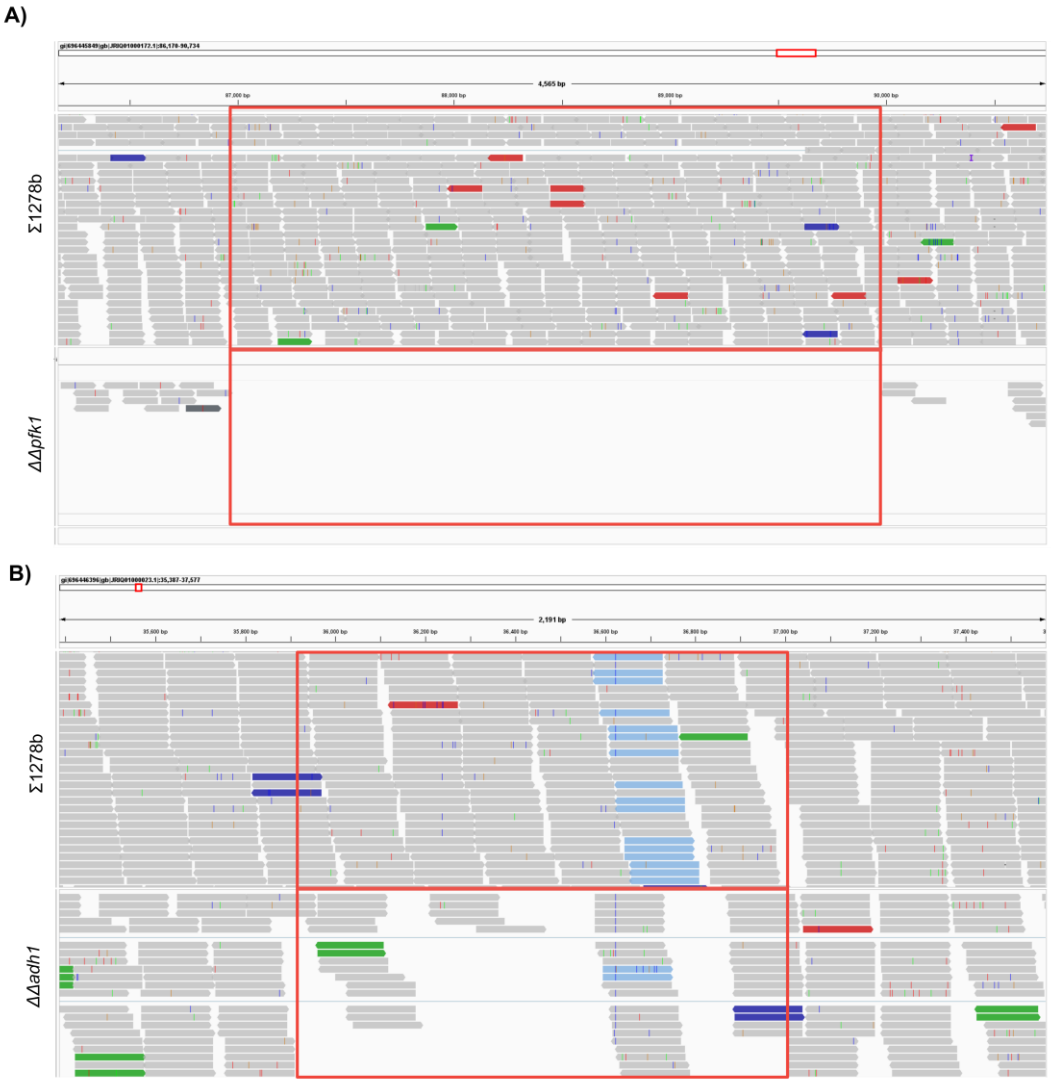

Figure Supplement 1. Confirmation of *pfk1* and *adh1* Deletion in *S. cerevisiae*.

(A) Confirmation of *ΔΔpfk1* strain using whole genome sequencing. IGV software was used for data visualisation. Red box represents gene locus of *pfk1* in wild-type (∑1278b) and *ΔΔpfk1* strains. **(B)** Confirmation of *ΔΔadh1* strain using whole genome sequencing. IGV software was used for data visualisation. Red box represents gene locus of *adh1* in wild-type (∑1278b) and *ΔΔadh1* strains. This figure was created using Biorender.com

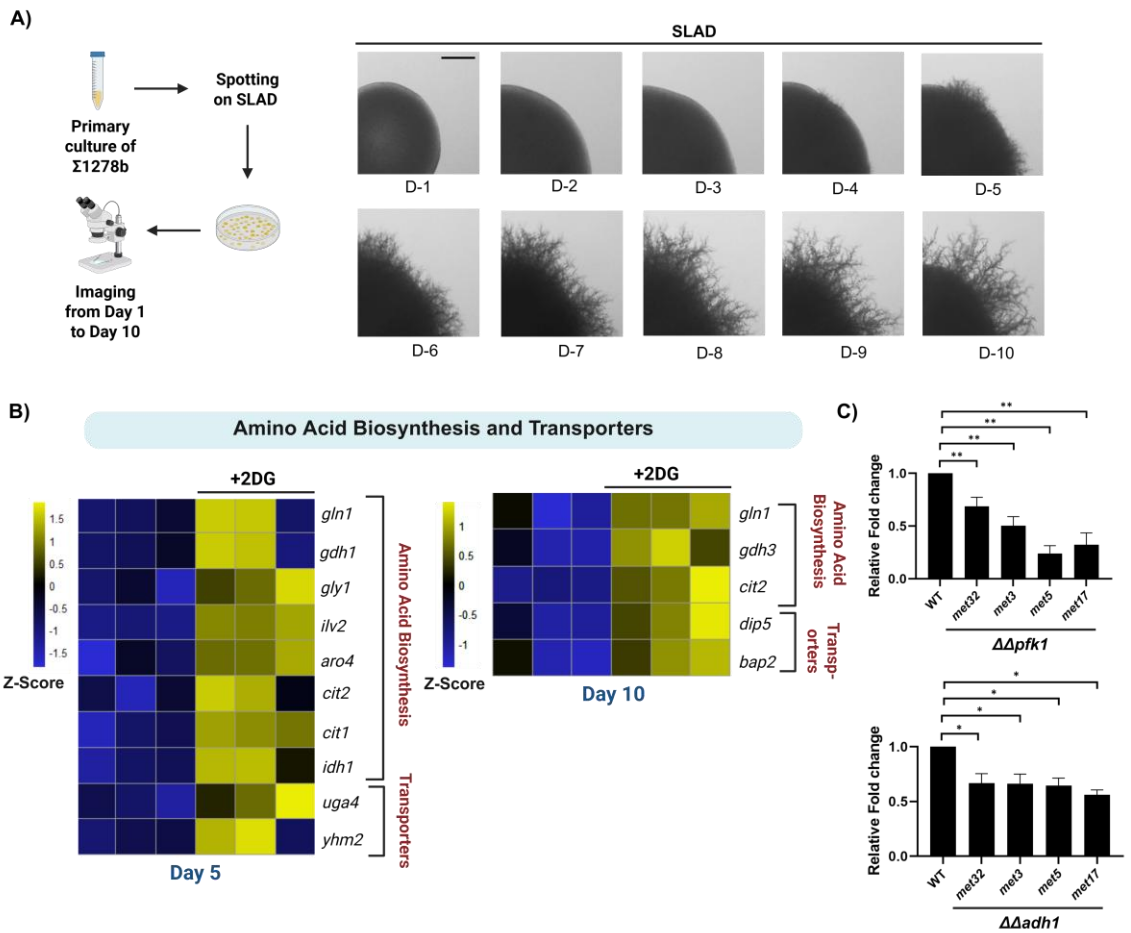

Figure Supplement 2. Comparative Transcriptomics Identifies the Role of Glycolysis During Pseudohyphal Differentiation in *S. cerevisiae*.

(A) Wild-type ∑1278b was spotted on SLAD, incubated for 10 days at 30 °C. Colonies were imaged every day, for 10 consecutive days (D-1 to D-10). Scale bar represents 1mm for whole colony images. **(B)** Heatmaps represent the differentially expressed genes involved in amino acid biosynthesis and transporters, in 2DG treated cells compared to untreated cells isolated from D-5 and D-10 colonies, respectively (n=3). Scale bar represents Z-Score. **(C)** *ΔΔpfk1* and *ΔΔadh1* along with Wild-type ∑1278b were spotted on SLAD and cells from colonies were isolated after ~4 days, for RNA isolation. We then performed comparative RT-qPCR to check for the relative expression of genes involved in the *de novo* biosynthesis of sulfur-containing amino acids pathway including *met32*, *met3*, *met5* and *met17.* Statistical analysis was done using one-way ANOVA test, **(P<0.01) and *(P<0.05). Error bars represent SEM. This figure was created using Biorender.com

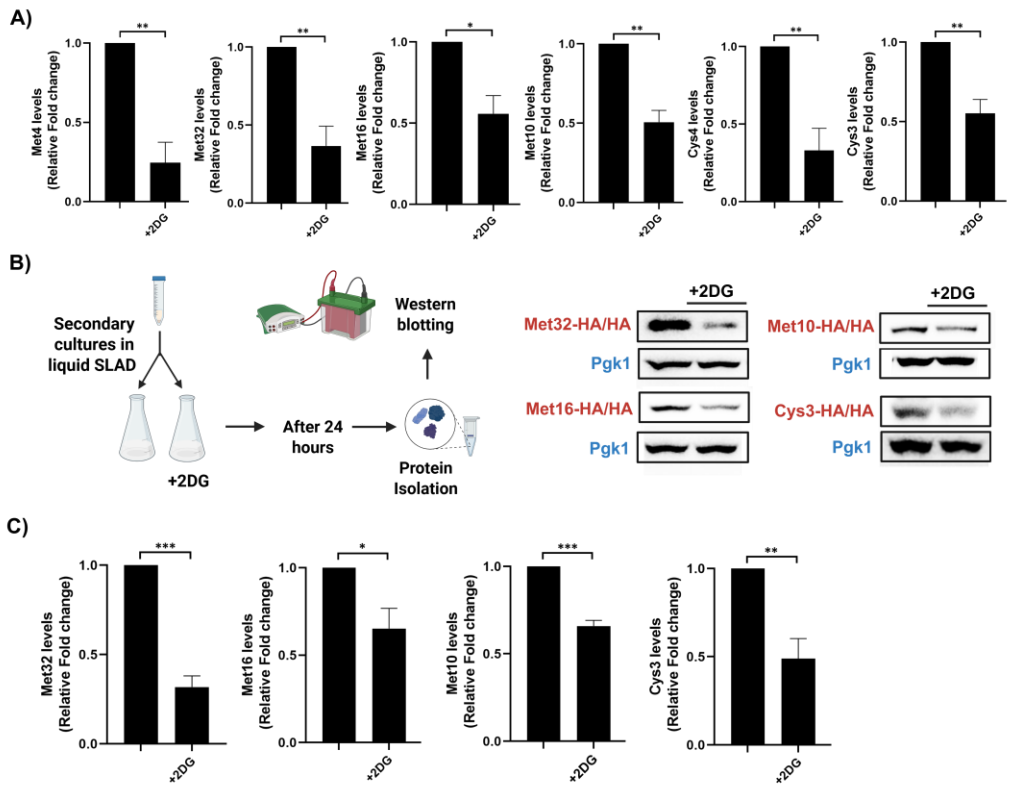

Figure Supplement 3. Expression of Proteins Involved in the *de novo* Biosynthesis of Sulfur-containing Amino Acids in Response to Glycolysis Perturbation.

(A) Epitope-tagged strains of various proteins involved in the *de novo* biosynthesis of sulfur-containing amino acids including Met4, Met32, Met16, Met10, Cys4 and Cys3 were spotted on SLAD in the presence and absence of sub-inhibitory concentration of 2DG following which, cells from colonies were isolated at day 5 and levels of these proteins were assessed using Western blotting. Raw images of Western blots were analysed using ImageJ to normalize targeted protein expression with the expression of housekeeping protein- β-actin, in order to generate densitometric graphs. Statistical analysis was done using unpaired t-test, **(P<0.01) and *(P<0.05). Error bars represent SEM. **(B)** Epitope-tagged strains of various proteins involved in the *de novo* biosynthesis of sulfur-containing amino acids including Met32, Met16, Met10 and Cys3 were grown in liquid SLAD and then treated with sub-inhibitory concentration of 2DG for 24 hours after which protein expression was checked using Western blotting. Pgk1 was used as loading control. **(C)** Raw images of Western blots were analysed using ImageJ to normalize targeted protein expression with the expression of housekeeping protein- Pgk1, in order to generate densitometric graphs. Statistical analysis was done using unpaired t-test, ***(P<0.001), **(P<0.01) and *(P<0.05). Error bars represent SEM. This figure was created using Biorender.com

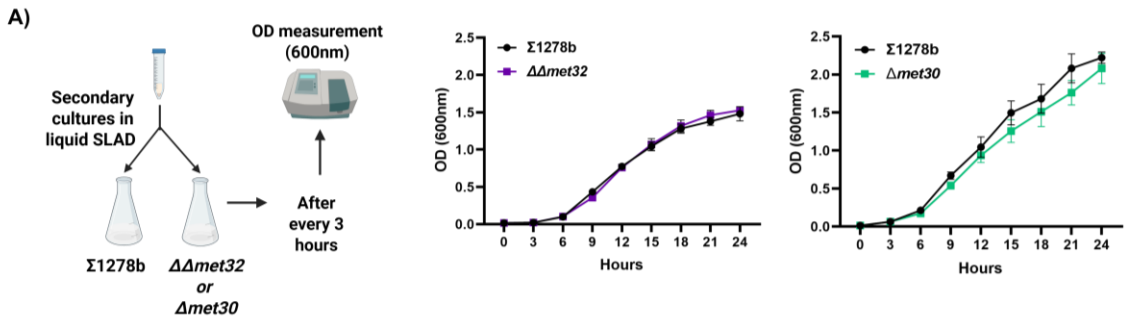

Figure Supplement 4. Monitoring of Overall Growth Rate of *ΔΔmet32* and *Δmet30* Strains.

(A) Growth curve analysis was performed to monitor overall growth of wild-type and *ΔΔmet32* strain as well as wild-type and *Δmet30* strain on SLAD. Overnight grown cultures of deletion strains (*ΔΔmet32* or *Δmet30*) along with wild-type strain (Σ1278b) were diluted to OD_{600}=0.01 in fresh SLAD and allowed to grow at 30 °C for 24 hours. OD_{600} was recorded at 3-h intervals. This figure was created using Biorender.com

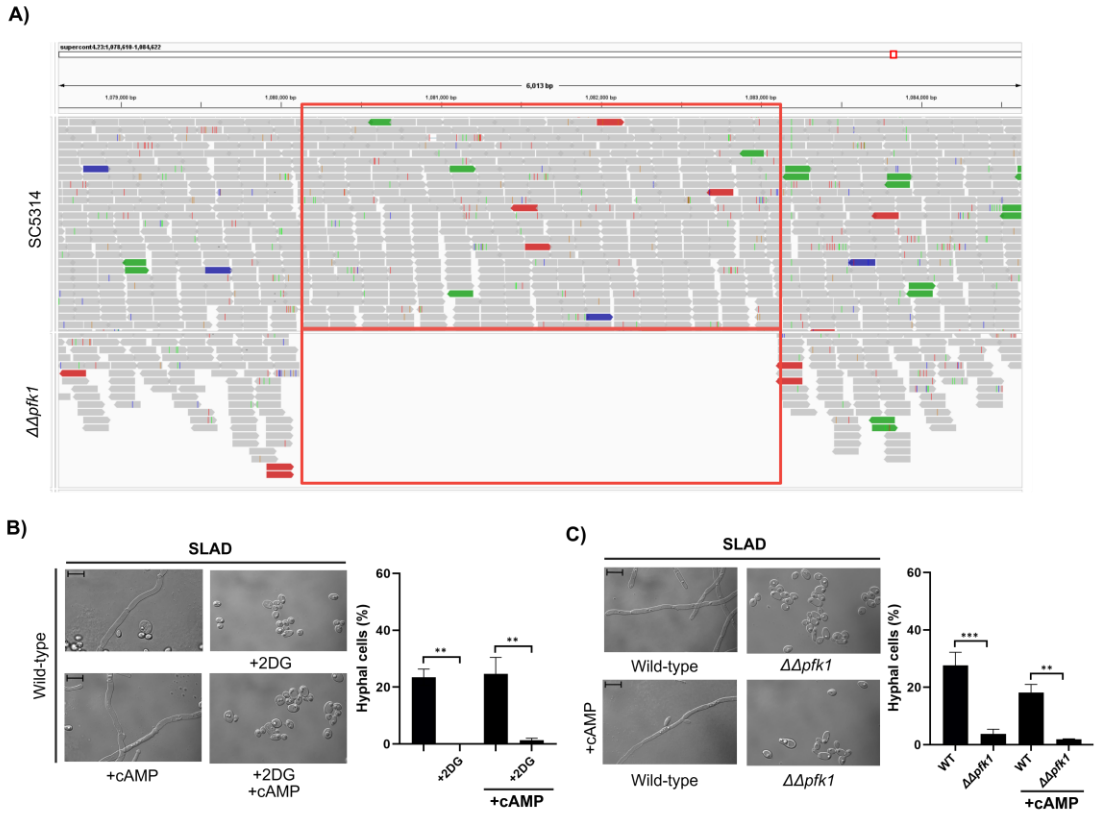

Figure Supplement 5. Confirmation of *pfk1* Deletion in *C. albicans* and Glycolysis is Critical for Hyphal Differentiation in a cAMP-PKA Independent Manner in *C. albicans*.

(A) Confirmation of *ΔΔpfk1* strain using whole genome sequencing. IGV software was used for data visualisation. Red box represents gene locus of *pfk1* in wild-type (SC5314) and *ΔΔpfk1* strains. **(B)** Wild-type SC5314 was spotted on SLAD containing sub-inhibitory concentration of 2DG with and without cAMP (5mM), incubated for 7 days at 37 °C. Cells from colonies were isolated and length/width ratio of individual cells was measured using ImageJ and percentage of hyphal cells from total population was determined. More than 500 cells were counted for each condition. Scale bar represents 10μm for single cell images. Statistical analysis was done using one-way ANOVA test,

2052 **(P<0.01). Error bars represent SEM. **(C)** Pertinent knockout strain which lacks the gene that
2053 encodes for the glycolytic enzyme phosphofructokinase-1 (*pfk1)* was spotted on SLAD with and
2054 without cAMP (5mM), along with wild-type and incubated for 7 days at 37 °C. Cells from colonies
2055 were isolated and length/width ratio of individual cells was measured using ImageJ and percentage
2056 of hyphal cells from total population was determined. More than 500 cells were counted for each
2057 condition. Scale bar represents 10μm for single cell images. Statistical analysis was done using one-
2058 way ANOVA test, ***(P<0.001) and **(P<0.01). Error bars represent SEM. This figure was created
2059 using Biorender.com
2060
2061 **Supplemental Table 1. Yeast Strains Used in this Study**
2062

Strain	**Genotype**
***S. cerevisiae* Σ1278b**	
Wild-type	*MATa/α*
SV18	*Δadh1::G418/Δadh1::HygB MATa/α*
SV21	*Δpfk1::HygB/Δpfk1::G418 MATa/α*
SV270	*Δmet32::NAT/Δmet32::G418 MATa/α*
SV320	*MET32-HA::G418/MET32-HA::NAT MATa/α*
SV394	*CYS3-HA::NAT/CYS3-HA::G418 MATa/α*
SV395	*CYS4-HA::NAT/CYS4-HA::G418 MATa/α*
SV402	*MET10-HA::NAT/MET10-HA::G418 MATa/α*
SV404	*MET16-HA::NAT/MET16-HA::G418 MATa/α*
SV451	*MET30-HA::NAT/MET30-HA::G418 MATa/α*
SV461	*MET4-HA::NAT/MET4-HA::G418 MATa/α*
SV463	*Δmet30::HygB/MET4-HA::NAT/MET4-HA::G418 MATa/α*
SV473	*MET16-HA::NAT/MET16-HA::G418/Δmet30::HygB MATa/α*
SV475	*MET32-HA::G418/MET32-HA::NAT/Δmet30::HygB MATa/α*
SV476	*CYS3-HA::NAT/CYS3-HA::G418/Δmet30::HygB MATa/α*
***S. cerevisiae* CEN.PK**	
Wild-type	*MATa/α*
SV109	*Δadh1::G418/Δadh1::NAT MATa/α*
SV117	*Δpfk1::NAT/Δpfk1::G418 MATa/α*
***C. albicans* SC5314**	
Wild-type	*MATa/α*
SV308	*Δpfk1::FRT/Δpfk1::SAT-FLP MATa/α*

2063
2064 **Supplemental Table 2. Oligonucleotides Used in this Study**
2065

Oligonucleotides	Sequence (5′ to 3′)
Primers for *S. cerevisiae* Gene Editing and Genotyping	
ADH1 KO F1	AGCTATACCAAGCATACAATCAACTATCTCATATACAATGCGGATCCCCGGGTTAATTAA
ADH1 R1	ATTTAATAATAAAAATCATAAATCATAAGAAATTCGCTTAGAATTCGAGCTCGTTTAAAC
ADH1 KO Chk	CGTTGTTGTCTCACCATATC
PFK1 KO F1	TTTTATATAAAAAATCTGAAACAAAATCATATCAAAGATGCGGATCCCCGGGTTAATTAA
PFK1 R1	CTCCTTTTGCTTAACTTAAACTTTTCATTGCAATCATTCAGAATTCGAGCTCGTTTAAAC

PFK1 KO Chk	AGGATGAGAAAGTGAAATCG
MET32 KO F1	AAGTCAAGAGGTATTATAAATTTCAAAAAAGTACCAAATGCGGATCC CCGGGTTAATTAA
MET32 R1	ATTTTCTTATTTGAGAAGATACACGCTATTTACTCTTTCAGAATTCGA GCTCGTTTAAAC
MET32 KO Chk	GATGGTTTTTCGTCCCTTAC
MET32 C tag F1	TCATCGTCAAGATAACAACCACAATGGTAGCAGTAATGGCCGGATCC CCGGGTTAATTAA
MET32 C tag Chk	GATGGTTTTTCGTCCCTTAC
CYS3 C tag F1	TTTGGAAGACATCAAGCAAGCCTTGAAACAAGCCACCAACCGGATCC CCGGGTTAATTAA
CYS3 R1	AAAGGTCCGGTCGAAGGCAGAGACGTGGCACTGGCGATTAGAATTC GAGCTCGTTTAAAC
CYS3 C tag Chk	CAGAGGTTTGAAGACTTTGC
MET10 Ctag F1	AGAATTAAAGGAAGCATCAAGATACATTTTAGAAGTCTACCGGATCC CCGGGTTAATTAA
MET10 R1	ACTGCTTTTCCTCGAGGTCACCCAAATATACAACGAGATGCGGATCC CCGGGTTAATTAA
MET10 Ctag Chk	TGGTTTAGGTACTGGTTTGG
MET16 Ctag F1	TGAAGCCAGCCGATTCGCGCAATTTTTAAAGCAAGATGCCCGGATCC CCGGGTTAATTAA
MET16 R1	GTCACATACATATGGTTATATATCGTACTCTATCTATCTAGAATTCGA GCTCGTTTAAAC
MET16 Ctag Chk	AATACGGGGATTTCTTATGG
MET4 Ctag F1	AAGCTTAAAGAAGCAAATTTTTGAGAAGGTTCAGAAAGAACGGATCC CCGGGTTAATTAA
MET4 R1	TATATATATATATAATTAAACTGTATAGTCTGTTATTTTAGAATTCGAG CTCGTTTAAAC
MET4 Ctag Chk	GAGCCAACTTTAAATGCAAG
CYS4 Ctag F1	CCATATCGTTACTAAGATGGATTTACTGAGCTACTTAGCACGGATCC CCGGGTTAATTAA
CYS4 R1	TTCTATGTTTGCTTTTATTTGAAGCGTGGGTTCTTATTTAGAATTCGA GCTCGTTTAAAC
CYS4 Ctag Chk	TTAAGGAAACCGCTAAGGTC
MET30 KO F1	AGGGGTGTGTGTTTGGTGATTTATAAAGGAGAAGGGCATGCGGATC CCCGGGTTAATTAA
MET30 R1	CGGATGTTTTTGACCAAGAAAAGACCACACACAGGTCCTAGAATTCG AGCTCGTTTAAAC
MET30 KO Chk	AGAGATAACTGCAGGGTGTG
MET30 Ctag F1	ATTTGGGTGCGTAAAAATGTACAAATTCGATCTCAATGATCGGATCC CCGGGTTAATTAA
MET30 Ctag Chk	AGGATGACCCAACAATGAC
Primers for *C. albicans* Gene Editing and Genotyping	
Psfs2a PFK1 F1	ATTTGAATAGCTTTTTCTTATTATTGAATTCTTTAATTTATCGTTTATTG CAAACAATCAATTATTCCTTATTATTTTGGGCAGATAACGAATTAGAA ATGAAGTTCCTATACTTTCTAG

Psfs2a PFK1 R1	CAACACATTGAATTACATATATGAGTATAAAAAATCAAACTATACTGG GGACTACAAATCTTACTATTTTACACAACTCCTTATCTTCTGTTCTTCA TTTGAAGTTCCTATTCTCTAGAA
Psfs2a SAT-FLP F1	AACATTGGATGCTGAGAACC
Psfs2a SAT-FLP R1	GCACATAATGCTATTTTCTC
PFK1 ApaI UF1	GAGAGGGCCCGTGATGCCTAACTTCTTGGT
PFK1 SacII DR1	CTCTCCGCGGTAGGCTGAATTGCTCGTATG
PFK1 KO R1 Chk	GTACCAATTGAAGTACCACC
FRT F1	CTTTCTAGAGAATAGGAACT
FRT R1	AGTTCCTATTCTCTAGAAAG
Primers for RT-qPCR	
S. cerevisiae ACT1 F1	CGTCTGGATTGGTGGTTCTATC
S. cerevisiae ACT1 R1	GGACCACTTTCGTCGTATTCTT
S. cerevisiae MET32 F1	TCCTCAATGTGGCAAAGGT
S. cerevisiae MET32 R1	CACCACCCGCAGTTAGTAAT
S. cerevisiae MET3 F1	CAGAGTTGAGACGCCGTTTA
S. cerevisiae MET3 R1	GTCTTGGTGGGTTGGATTCT
S. cerevisiae MET5 F1	CATCGCCGTTCCTCCATATAAC
S. cerevisiae MET5 R1	CCCATACCACCACCAACAAA
S. cerevisiae MET17 F1	CCCTGGTTTAGCATCTCATTCT
S. cerevisiae MET17 R1	CAGTTTCCTTGTCGGCATTTG
C. albicans ACT1 F1	TTGGATTCTGGTGATGGTGTTA
C. albicans ACT1 R1	TCAAGTCTCTACCAGCCAAATC
C. albicans MET32 F1	CACCAACACAACACCATCAAC
C. albicans MET32 R1	TCCAATTCCACCACCAGTAATC
C. albicans MET3 F1	GTTCCAACAACAAACCCAACTC
C. albicans MET3 R1	TCACCATCAGCATTACCAGAAG
C. albicans MET5 F1	TTTATGGTGCGTGTTCGTTTAC
C. albicans MET5 R1	TAGCCCTGGTGGTCAATTTC
C. albicans MET10 F1	GGGTTGATCCAAAGGGAAGAT
C. albicans MET10 R1	GACAATGGTGGCAACTTCATAAC
C. albicans MET17 F1	TCAAGGACATCACCAACACC
C. albicans MET17 R1	CTTAGAGTCACCCACATTAGCC
C. albicans ALS3 F1	GGTGGCACTGATTCGGTTAT
C. albicans ALS3 R1	GCGGTAATGGTAGTGGTAGTTG
C. albicans ECE1 F1	TTGGCAACATTCCACAAGTAATC
C. albicans ECE1 R1	CAGCAATGATACCAGCAACAAC
C. albicans HWP1 F1	CTCTACGACTGAAGGTGCTATTC
C. albicans HWP1 R1	GTAGAAATAGGAGCGACACTTGA
C. albicans HYR1 F1	CACATCAAGTCCTGGTCAATCTA
C. albicans HYR1 R1	TGGAACAGTGGTGAAGATAGTG
C. albicans IHD1 F1	GGCTCTCAAGGTCAATCTACAA

C. albicans IHD1 R1	ACTAGCACCATCGTTACCATTAG
C. albicans RBT1 F1	CCATCTGCTAACTCCTCATACAC
C. albicans RBT1 R1	CAAGAATGCAGCAAGACCAATAA
C. albicans SAP6 F1	GAGTGTTCTTGCTTTCGCTTTAT
C. albicans SAP6 R1	CATCTGGATCAACAAGGGATCT

2066
2067 **Supplemental Table 3. List of Reagents and Tools Used in this Study**
2068

Reagents/ Resource	Reference or Source	Identifier or catalog Number
Recombinant DNA		
pFA6a-kanMX	Gift from Dr. Sunil Laxman	Not applicable
pFA6a-Hyg	Gift from Dr. Sunil Laxman	Not applicable
pFA6a-Nat	Gift from Dr. Sunil Laxman	Not applicable
pFA6a-Ctag-HA-G418	Gift from Dr. Sunil Laxman	Not applicable
pFA6a-Ctag-HA-NAT	Gift from Dr. Sunil Laxman	Not applicable
pSFS2a-NAT	Gift from Dr. Kaustuv Sanyal	Not applicable
Antibodies		
Rabbit anti-HA	Cell Signaling Technology	3724S
Mouse anti-β-actin	Cell Signaling Technology	3700
Mouse anti-PGK1	Santa Cruz Biotechnology	sc-130335
Goat anti-Rabbit IgG-HRP conjugate	Cell Signaling Technology	7074S
Horse anti-Mouse IgG-HRP conjugate	Cell Signaling Technology	7076S
Chemicals, enzymes and other reagents		
BD Bacto agar	Becton Dickinson	214010
Agarose	MP Biomedicals	100267
Ammonium sulfate	Sisco Research Laboratories	0149175
Blotto, non-fat dry milk	Santa Cruz Biotechnology	sc-2324
B-mercaptoethanol	Sigma-Aldrich	444203
Diluent	HiMedia	MB228
D-(+)-Glucose anhydrous	HiMedia	GRM016
Lithium acetate	Sigma-Aldrich	517992
Peptone	Thermo Fisher Scientific	211677
RNaseZAP	Sigma-Aldrich	R2020
SDS	G Biosciences	RC1184
Trichloro acetic acid	Sigma-Aldrich	100807
Tris, free base	HiMedia	MB029
Tween 20	Sigma-Aldrich	P7949
Yeast extract	Thermo Fisher Scientific	212750
Yeast nitrogen base w/o amino acids and ammonium sulfate	Becton Dickinson	233520
L-Cysteine	Sigma-Aldrich	30089
L-Methionine	Sigma-Aldrich	64319
Sodium citrate	Sigma-Aldrich	C8532

Glycerol	HiMedia	MB060
Potassium acetate	MP Biomedicals	191425
2-Deoxy-D-Glucose	Sigma-Aldrich	D8375
NAT	Jena Bioscience	AB-102XL
G418	MP Biomedicals	158782
Ethidium bromide	HiMedia	MB074
Pico-ECL substrate	Thermo Fisher Scientific	34579
Femto-ECL substrate	Thermo Fisher Scientific	34094
TEMED	Sisco Research Laboratories	52145
Hygromycin	Sigma-Aldrich	H0654
Ribopure RNA purification kit-Yeast	Thermo Fisher Scientific	AM1926
BCA Protein Assay kit	Thermo Fisher Scientific	23227
GMS Staining kit	ABcam	AB287884
Softwares		
RStudio v4.3.2	Posit	Not applicable
GraphPad Prism v9	GraphPad software	Not applicable
ImageJ		Not applicable
IGV v2.16.2		Not applicable
Other		
Glass beads	HiMedia	GRM2228
MATRIX thermoshaker	IKA	Not applicable
Spectrophotometer	Thermo Fisher Scientific	Not applicable
Proflex PCR systems	Thermo Fisher Scientific	Not applicable
MVX10 Stereo Microscope	OLYMPUS Scientific	Not applicable
Biosafety Cabinet	IGene Labserve	Not applicable
PVDF membrane	Milipore	IPVH00010
Mini Trans-Blot Cell Module	Bio-Rad	Not applicable
ChemiDoc™ MP analyzer	Bio-Rad	Not applicable
QuantStudio 5 Real-Time PCR System	Thermo Fisher Scientific	Not applicable
Apotome widefield fluorescence microscope	Zeiss	Not applicable
Centrifuge 5425R	Eppendorf	Not applicable

2069